Utrecht University

Impacts of climate change on debris flow frequency and magnitude in high mountain Asia

Master Thesis: Leon Duurkoop
Student nr.: 6935737

Supervisor: W.W. Immerzeel
Second supervisor: V. Bazilova
Geosciences Utrecht University, 2024

Abstract

Debris flows are a mixture of large amounts of sediment and water which are moving at high speeds. These types of mass movements are a common occurrence in High Mountain Asia (HMA) and can be very hazardous for the population. It is expected that climate change will influence the frequency and magnitude of debris flows due to changes in the availability of water and sediment associated with retreating glaciers, mountain greening, and changes in precipitation and temperature. However, there is a considerable amount of uncertainty about what the effects of climate change will be. Some studies have shown that climate change will decrease the frequency and magnitude of debris flows due to drier and warmer conditions. While others have shown an increase in debris flow magnitude and frequency due to shifts in precipitation and increased sediment availability due to weathering and glacier retreat. This study aims to quantify the effect of different parts of climate change in combination with land cover changes for 3 regions in HMA with very different climates: Bagrot valley (Pakistan/Karakoram), the Mustang district (Nepal/Himalaya) and Langtang Valley (Nepal/Himalaya). This study will be looking at transport-limited systems and will be done by using an extended version of the Sediment Cascade model (SedCas), introducing a 3rd hydrological response unit for glaciated areas adding on to the other two (vegetation and bedrock). Overall, it becomes clear that a vegetation increase results in a decrease in debris flow activity. The same is true for glacier decrease. Changes in precipitation extremes have been identified as an important factor and depending on if they increase or decrease, debris flow frequency and magnitude change in the same manner. Temperature increases show a more indirect effect, mostly affecting the amount of snow cover days and the elevation at which there is permanent snow cover present, resulting in increases in debris flow magnitude and frequency due to lack of snow cover. This study shows that changes in these climate factors are not consistent across HMA resulting in Bagrot having an increase in debris flow magnitude and frequency while Langtang sees an overall decrease during the time periods looked at (1951-2022). Mustang has a very large variability in response to climate change, having areas with an increase as well as areas with a decrease. This study gives a better understanding of the effect that the changing climate has on debris flow activity. For future studies it would be of interest to also look at supply-limited systems and at future climate projections to further this understanding. This better understanding can help the population of areas prone to debris flows to better adapt to these hazardous mass movements.

Table of Contents

1. Introduction

Due to climate change, conditions in High Mountain Asia (HMA) are changing, with temperatures rising and precipitation patterns shifting (Lalande et al., 2021). Due to this warming and the changes in precipitation the glaciers that are located there are retreating (Hugonnet et al., 2021; Sakai & Fujita, 2017). The retreat of these glaciers and the overall changes in climate are expected to have an impact on the frequency and magnitude of mass movements due to changes in water availability in the catchment and destabilization of the moraines, introducing loose sediment into the system (Ban et al., 2020; Hirschberg et al., 2021). An increase in the frequency or magnitude of mass movements can have a large impact on the millions of people living downstream of a glacier (Karakaş & Coruk, 2011).

Mountainous areas like HMA experience many types of mass movements involving large amounts of water and sediment. A significant amount of these mass movements takes place as debris flows. Rapp (1960) found that on the mountain slopes of Kärkevagge (Sweden) between 1952 and 1960 around 46% of the sediment was displaced by debris flows. It has also been stated that around 30% of fatalities during heavy rainstorms in Japan are caused by debris flows (Takahashi, 1981), which on its own stresses the importance of more research into how these mechanisms work. Debris flows distinguish themselves from other mass movements like sediment floods and rock avalanches by the fact that both the liquid and solid forces influence their rheological properties. Rheological properties are the characteristics of a material that describes how it flows or deforms in response to applied forces (Costa, 1988; Iverson, 1997; "Rheological Properties," 2007). Debris flows typically contain between 20% to 60% water, the larger flows can surpass a volume of 1 km^3, can have a runout distance that is longer than 100.000 m and can reach peak velocities that exceed 10 m/s (Costa, 1988; Pierson, 2005; Iverson, 1997).

Debris flow catchments can generally be classified as supply-limited, or transport-limited (supply-unlimited) (Jakob, 1996; Bovis & Jakob, 1999). In transport-limited catchments the limiting factor for a debris flow to occur is the amount of water that is available. Contributors to this total amount of water can be just rainfall, however, they can also include other sources like snow melt or glacier melt. In this type of catchment there is enough sediment available for a debris flow to occur, however, it needs a large amount of rainfall or other water source to trigger a debris flow (Bovis & Jakob, 1999). Furthermore, in a transport-limited catchment the amount of rainfall that triggers a debris flow is not fixed but may depend on the volume of sediment available (Brayshaw & Hassan, 2009). In a supply-limited system, the limiting factor for a debris flow to occur is the sediment recharge rate. In this type of catchment there is always enough water available when it rains, however, sediment must recharge up to a large enough volume for a debris flow to occur (Figure 1) (Montgomery & Bierman, 2013).

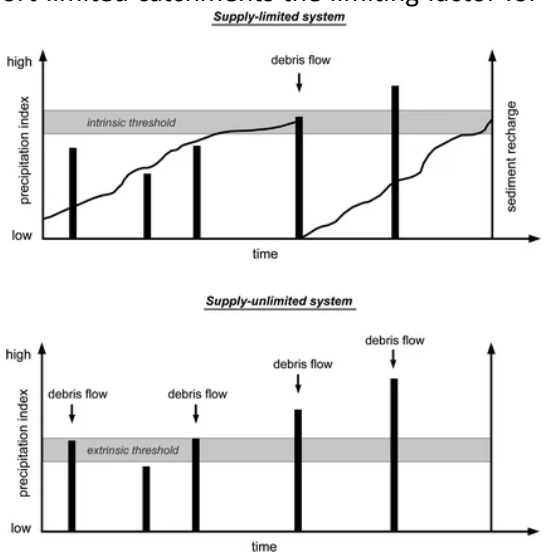

Figure 1: Illustration of a Supply-limited system and a Supply-unlimited system (Bovis & Jakob, 1999)

Most glaciers in high mountain Asia have been recessing since the end of the Little Ice Age (LIA), changing the landscape from glacial to periglacial conditions which influences the sediment and hydrological dynamics significantly (Haeberli, 2013; Seppi et al., 2015). Slope processes on the flanks of melting moraines (gully and rill erosion) accumulate large amounts of debris. Just like the melting of glaciers leaves large amounts of unconsolidated material. All this loose material can be picked up by and feed debris flows that are triggered by large amounts of rainfall or a sudden release of water such as sub-glacial outbursts or glacial lake outburst floods (Legg et al., 2014). The water availability in the catchment therefore is also a key factor in mass movements like debris flows. This also experiences change due to more, less, or more irregular precipitation and the way in which the precipitation falls, i.e., snow or rain (Harrison et al., 2021; Singh et al., 1997). When snow accumulates in the channel it can hinder bedload sediment transport, therefore accumulating debris in the catchment that will be released when melting starts (Hirschberg et al., 2021). However, shorter snow-covered periods and increased rainfall can also increase the chance of debris flows (Fort, 2014). Snow cover insulates bedrock, therefore maintaining a stable ground surface temperature and slowing down weathering by decreasing the effect of thermal expansion (Salzmann et al., 2007). So, when snow cover and subsequently its insulating effect disappear, sediment production might go up. The enhanced melting of glaciers also introduces a significant amount of water into the system. This amount fluctuates over time because of increased or decreased melting due to climate change and seasonality (Nie et al., 2021; Verbunt et al., 2003). An increase or decrease in vegetation cover due to climate change in periglacial environments can also have an effect on the two driving factors in debris flow mechanic that Bovis & Jakob (1999) describe. An increase in vegetation can slow down periglacial processes like gullying and rill erosion by trapping the sediment, reducing sediment availability in a basin (Eichel et al., 2016). Over time this might decrease debris flows. On the other hand, a decrease in vegetation cover due to drier conditions can destabilize areas in the basin and can make it more prone to landslides that feed debris flows. Vegetation also plays an important role on water availability in a catchment effecting evapotranspiration (Wang et al., 2014). Therefore, increases or decreases in vegetation cover due to climate change could have an impact on debris flow frequency and magnitude. There is the expectation that HMA will experience mountain greening because of climate change due to three main driving factors: Increases in precipitation, decreases in snow cover and increases in irrigation by local population (Maina et al., 2022).
However, quantifying the response of debris flows to climate change remains a difficult task due to the many different relationships between the different components that drive debris flows as described above (Gariano & Guzzetti, 2016).

In the past there have been many ways to monitor and quantify the magnitude and or frequency of debris flows; from pressure and vibration sensors to remote sensing (Itakura et al., 2005). Usually, this combination of different sensors and techniques is used to develop models that are able to quantify the magnitude and frequency of debris flows. There have been previous studies that used models to examen the sensitivity of basin sediment yield and even debris flow sediment yield in relation to climate change, more specifically related to landscape evolution, as we might see in the future in HMA when going from glaciated areas to periglacial conditions with more vegetation (Coulthard et al., 2012; Istanbulluoglu, 2009; Perron, 2017; Hirschberg et al., 2021). And therefore, modelling might be an adequate way to quantify the effects of climate change on the frequency and magnitude of debris flows (Hirschberg et al., 2021).

Like the observational methods, debris flow modelling remains challenging, however, it also opens up new possibilities. Debris flows can have a very low frequency and high velocity, therefore, observing takes a long time and can be very hard. However, with models one can simulate long

periods and therefore analyse the frequencies and magnitudes of debris flows, which is not possible with observations due to the generally long recurrence periods. Modelling also allows you to conduct experiments and systematically change parameters and variables to understand the drivers and underlying processes of debris flows. Depending on the goal of the study there are a few things to consider. For example, if the model should be spatially distributed or lumped and if the model should be empirically or physically based. A physically spatially resolved model needs a lot of high-resolution data as input which is not always available and can take a long time to process. Therefore, empirical models can be better to work with because they are computationally more efficient than physically based models. However, these models provide less understanding of a system due to lack of fundamental physical principles and are solely based on statistical analysis. There are, however, models that sit in between these two types of models called conceptual models or grey-box models. These are spatially lumped models that use highly simplified physical laws based on observed or assumed empirical relations. These models do not need large amounts of data and are therefore more friendly to use but still give a physical understanding of the processes (Liu et al., 2017).

Bennett et al. (2014) and Hirschberg et al. (2021) developed such a model: a probabilistic sediment cascade model (SedCas) used to simulate sediment transfer in mountain basins. The model was designed to better understand the dynamics between sediment transport and production. It was originally made for the Illgraben catchment in Switzerland. Hirschberg et al. (2021) used it to model the response of the Illgraben catchment to climate change and found that for the projected changes in precipitation and air temperature there will be a reduction in both sediment yield (−48%) and debris-flow occurrence (−23%). This reduction is due to reduced freezing, limiting frost-weathering and reducing the amount of material in the catchment. If the Illgraben would be a supply-unlimited system the changes in climate would have increased future sediment yield by 23% in the short term (2035), 31% in the midterm (2060), and 48% in the long term (2085) (Hirschberg et al., 2021). Illgraben does not have glaciation, which would introduce meltwater and large amounts of material changing the dynamics of the system. Subsequently, this study is only relevant for catchments in mountainous areas without glaciation. Therefore, in this study SedCas has been extended to consider glaciers and better represent other types of catchments as located in HMA. This study will apply the SedCas modelling framework to different parts of HMA, with contrasting climate regimes.

The aim of this study is to quantify the impacts of climate change on debris flow frequency and magnitude in different parts of High Mountain Asia using the SedCas model.

The objectives for this study are:

1. Quantifying the effects of changing water availability due to changing climate (changes in precipitation but also in glacier output) in the catchments in High Mountain Asia on the frequency and magnitude of debris flows.
2. Quantifying the effects of changing landscape, moving from glacial to periglacial conditions to more vegetated conditions, on the frequency and magnitude of debris flows.
3. To evaluate whether climate change impacts on debris flow occurrence and magnitude are consistent across different parts of high mountain Asia.

2. Study area

The focus of this study is High Mountain Asia, more specifically 3 different areas that have basins that are prone to debris flows and floods (Figure 2). The study areas are specifically chosen because of their contrasting climates. This way it is possible to get a more complete view of how climate change affects debris flows over high mountain Asia. The catchments are retrieved form Global Administrative Areas 2.0 (GADM) which is a project creating spatial data for many countries using databases provided by national government or organizations, or other maps and names available from the internet (*Global Administrative Areas*, 2012).

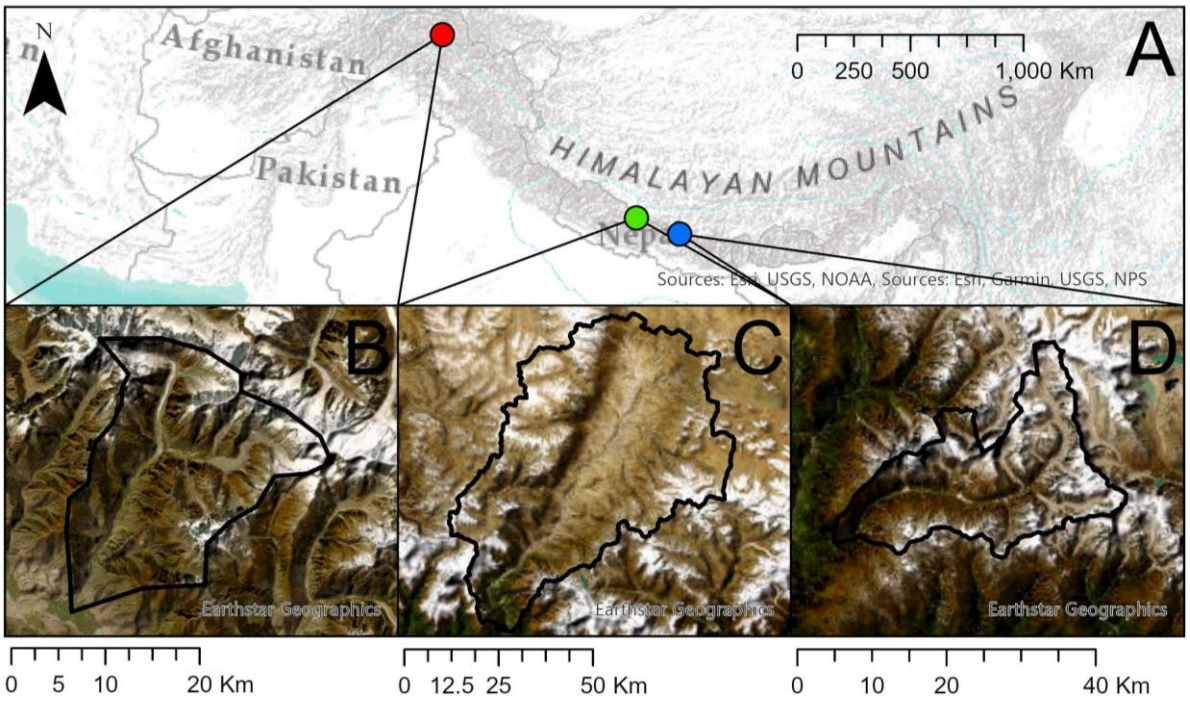

*Figure 2: A: Overview of HMA with study areas marked, B: Bagrot Valley, C: Mustang Valley, D: Langtang Valley (*Global Administrative Areas*, 2012).*

2.1 Mustang

The first area is the northern Mustang district in Nepal (3573 km^2) (Figure 2_C). This area is located north of Annapurna (8091 m) and Dhaulagiri (8172 m). As a result, it lays in the rain shadow of these mountains and is relatively protected from influences of the monsoon, resulting in a semi-arid and continental climate. Due to this semi-arid climate vegetation is only sparse. The climate is representative for a significant part of HMA called the Trans Himalayan zone (Fort, 2014). There is high temperature variability in the area due to large elevation changes. And there is also large interannual precipitation variability resulting in 'wet' years and 'dry' years with the 'wet' years (300 mm) having three times more precipitation on the valley floor then the 'dry' years (100 mm). During winter and above an elevation of 2500 m most of the precipitation falls in the form of snow (Fort, 1996). The valley has only sparse remains of glaciation despite being located in close proximity to Annapurna and Dhaulagiri. The valley floor is free of glaciation and the lower most glacier tongue is found at an elevation of 3200 m, which is rather unusual compared to other parts of the Himalaya where glaciers have a larger presence (Fort, 2000) (Figure 3_A).

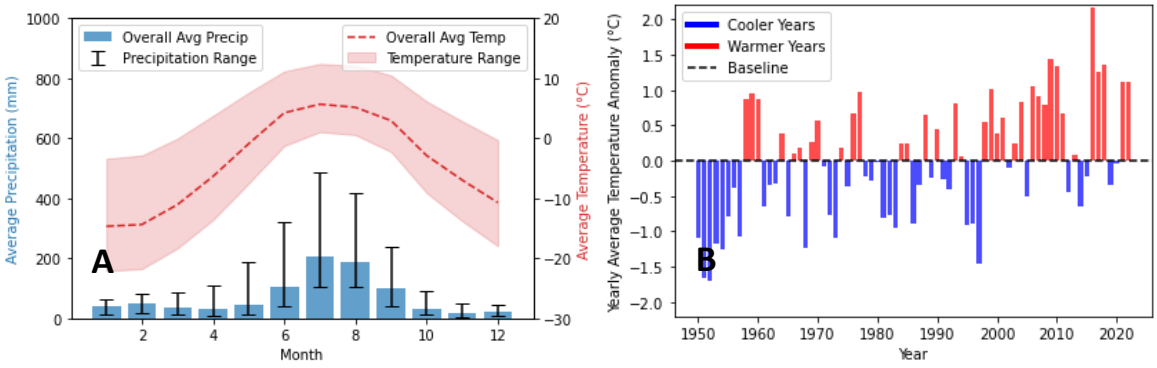

Figure 3: A: Climate Mustang based on ERA5-land data with variability between the different grid cells, B: Yearly average temperature anomaly 1951-2022 based on ERA5-land data average over all pixels in study area. See section 3.2 (Muñoz-Sabater et al., 2021).

2.2 Bagrot valley

Bagrot valley is the second area and is located in Central Karakoram National Park in Pakistan (Figure 2_B). Bagrot valley is one of the more geomorphic active areas in the Karakoram region and has an area of 374 km^2 (Calligaris et al., 2013). This part of HMA is more tectonically active, resulting in earthquakes that can suddenly supply a lot of sediment in the form of rock avalanches (Hewitt et al., 2011). The area has very extreme relief, with elevations ranging from 1500 m in the lowest point of the valley up to 7788 m at the summit of the highest mountain (Rakapoishi). This results in a very high variance in temperature due to the fast changes in elevation, just like in the Mustang district. For Bagrot valley precipitation also varies greatly with elevation. With very dry conditions in the lower parts of the valley (135 mm/y) and more humid conditions at higher elevation (720 mm/y). Above 5000 m, precipitation rates can be up to 2000 mm/y (Wake, 1989). 90% of this precipitation falls in the form of snow (Winiger et al., 2005). This, however, is not reflected in Figure 4 because of the coarse resolution of ERA5-land. The annual variation in precipitation is very different compared to Mustang, with all year-round precipitation and no clear wet or dry season (Figure 4).

Glaciation is far more extensive in Bagrot valley when compared to the Mustang region. Hinarche glacier alone covers almost 10% of the total area of the valley. This is the main glacier of the valley and extends from 7788 m al the way down to 2500 m. From 2500 to 3350 m the glacier is almost flat and extends over 9 km. From 3350 m to 7788 m the glacier is a steep icefall over a length of only 8.5 km. The Hinarche glacier is very representative for the other glacier valleys in Central Karakoram National Park (Mayer et al., 2010)

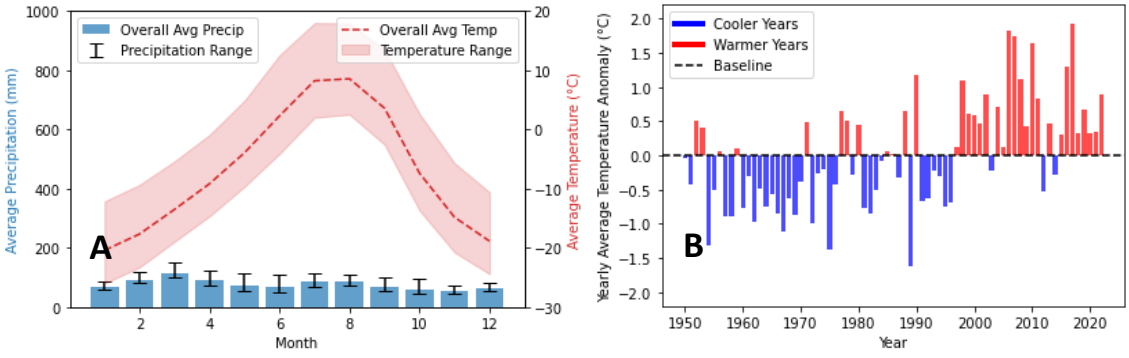

Figure 4: A: Climate Bagrot based on ERA5-land data with variability between the different grid cells, B: Yearly average temperature anomaly 1951-2022 based on ERA5-land data average over all pixels in study area. See section 3.2 (Muñoz-Sabater et al., 2021).

2.3 Langtang valley

Langtang valley has been chosen as the third study area, because this area has seen a lot more field observation compared to the other areas and has a contrasting monsoon dominated climate due to its location in the central Himalaya (Steiner et al., 2021). Langtang valley is located 60 km north of Kathmandu, Nepal. The area of Langtang valley is 584 km^2 (Figure 2_D). The valley has an elevation range from 1406 m to the highest mountain surrounding it, Langtang Lirung, which summit reaches 7234 m (Collier & Immerzeel, 2015). This areas climate is dominated by the monsoon which brings around 80% of the yearly precipitation in the valley (Lacroix, 2016). Precipitation in the valley peaks at an elevation of 3000 m and decreases almost linearly going up or down in elevation (Collier & Immerzeel, 2015). Seasonal changes in precipitation are very large in Langtang compared to Bagrot and have a closer resemblance to Mustang (Figure 3, 4 and 5). However, Langtang receives much more precipitation overall and with more seasonality. Glaciation starts at an elevation of 4040 m and covers 24% of the area of the valley. Below 3000 m the valley is densely forested which is in strong contrast to the other two catchments (Collier & Immerzeel, 2015).

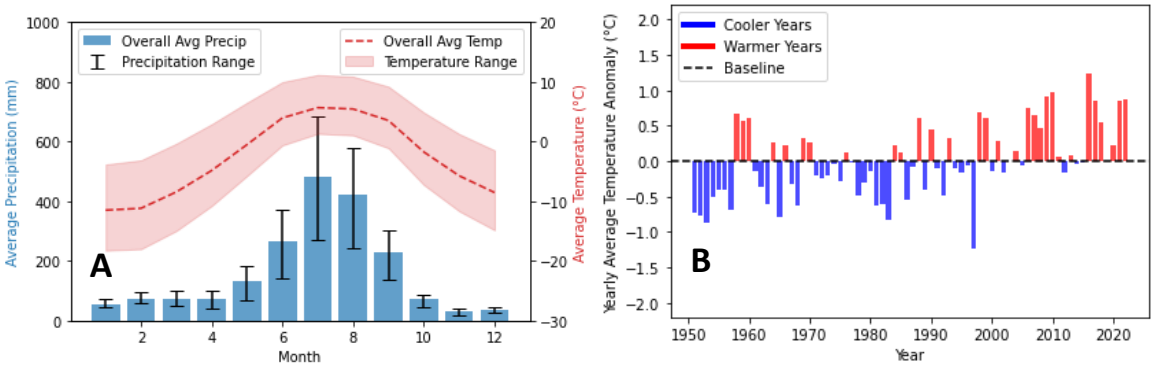

Figure 5: A: Climate Langtang based on ERA5-land data with variability between the different pixels grid cells, B: Yearly average temperature anomaly 1951-2022 based on ERA5-land data average over all pixels in study area. See section 3.2 (Muñoz-Sabater et al., 2021).

3. Data and methods

The Sediment Cascade Model (SedCas) has been modified to account for glacier melt and will be executed using ERA5 reanalysis data. The model was executed for 2 periods of 35 years with changing land cover and a change in climate. Hereby the assumption has been made that the catchments are supply-unlimited due to the assumption that the retreat of glaciers will introduce large amount of unconsolidated sediment, and therefore the focus will be on how the hydrological changes in the study areas will affect the magnitude and frequency of debris flows and overall sediment transport.

3.1 SedCas

For the study, the Sediment Cascade Model (SedCas) will be used. This model was developed by Bennett et al. (2014) and improved by Hirschberg et al. (2020). The model is spatially lumped and it combines two models: a sediment model and a hydrological model. The sediment model describes the movement of sediment from landslides to hillslopes to the channel. The hydrological model describes all the relevant hydrological processes that influence or generate runoff by simulating the water balance for the basin. These two models combined generate the water and sediment output of the basin in the form of debris flows or normal outflow. The timesteps of the model are hourly. A more in-depth explanation of the model can be found in Bennett et al. (2014) or Hirschberg et al. (2021). For application on catchments or basins with glaciers the model has been expanded in the form of an extra hydrological response unit (hru) for glaciers adding to the already existing hru for bedrock and vegetation. The hru simulates a melting glacier with snow on top, as a percentage of the total basin. The melt is generated based on a degree day model (Formula 1) that is adjusted for hourly data. This melt is added to the water balance as part of the hydrological model. The area covered by glacier does not produce any sediment. The degree day model has been used for snow melt in the original version of Sedcas and has been used for glacier melt in other studies and showed good results (Bennet et al.,2000; Singh et al., 2000). The DDF value for snowmelt is 0.08 mm/degrees Celsius and is calibrated for the Illgraben catchment. For glacier melt, the DDF is estimated based on literature. The DDF value for clean glaciers is 7±2 and a DDF value for debris covered glaciers is 2±2 mm/degrees Celsius (Immerzeel et al., 2015). For this model a weighted average of 6.5 mm/degrees Celsius is used, based on 10% of glaciers being debris covered in Central Asia (RGI zone 13) (Herreid & Pellicciotti, 2020). This value needs to be converted to hourly melt because of the hourly nature of the Sedcas model, resulting in a DDF of 0.27 mm/degrees Celsius.

$$M_h = DDF * (T_h - T_0) \; if \; T_h > T_0 \qquad (1)$$
$$M_h = 0 \qquad if \; T_h < T_0$$

Where:

- M_H is the hourly melt (mm)
- T_h is the hourly average temperature 2 meters above the surface (Degree Celsius)
- T_0 is the reference air temperature (usually 0 degree Celsius)
- DDF is an empirically derived factor in this case 0.27 mm/degrees Celsius.

All catchments will be modelled as transport limited systems. Therefore, the model will generate an output variable called Qdftl, which stands for Discharge from debris flow yield, transport limited. This is the discharge that is transported in the form of a debris flow.

3.2 Climate data

The Sedcas model is fed by hourly climate data (temperature, precipitation, short wave radiation and cloud cover) (Bennett et al., 2014). For this study climate data from ERA5 is used. For the years 1951 to 2022 temperature 2 m above the surface, total precipitation, surface solar radiation downwards and total cloud cover have been downloaded for the 3 different study areas. ERA5 is produced by the Copernicus Climate Change Service (C3S) at ECMWF (European Centre for Medium-Range Weather Forecasts) and is the fifth iteration of ECMWF atmospheric reanalysis of global climate (Muñoz-Sabater et al., 2021). ERA5 has been chosen because of its hourly timesteps that fit well with the input necessary for SedCas, its consistency with coverage around the globe and because it has successfully been used for climate change assessments in mountain regions before (Pepin et al., 2022, Kraaijenbrink et al., 2021, Bhattacharya et al., 2021). ERA5 has a spatial resolution of 0.25 degrees (≈31 km) grid spacing and will be used for cloud cover. The other 3 climate components necessary for SedCas come from ERA5-land which has a spatial resolution of 0.1 degrees (≈ 9 km) grid spacing (Table 1 & Figure 6). ERA5 also provides geopotential values for the grid pattern these are used to calculate the elevation for each grid cell.

Table 1: ERA5-land and ERA5 data (Muñoz-Sabater et al., 2021).

Data	Source	Resolution
Temperature (C°)	ERA5-land	0.1 ° (≈ 9 km)
Precipitation (mm)	ERA5-land	0.1 ° (≈ 9 km)
Short wave radiation (W/m²)	ERA5-land	0.1 ° (≈ 9 km)
Cloud cover (-)	ERA5	0.25 ° (≈31 km)

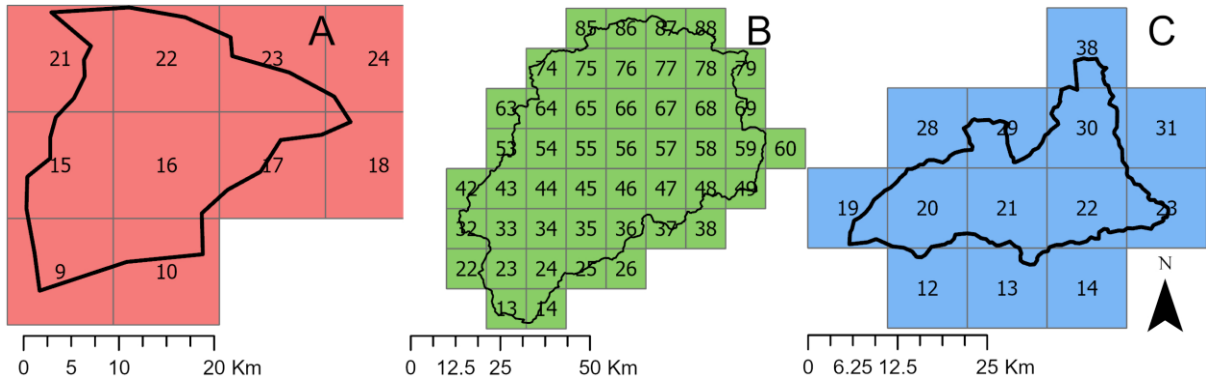

Figure 6: A: Overview of Bagrot Valley with the corresponding climate cells, B: Overview of Mustang Valley with the corresponding climate cells, C: Overview of Langtang Valley with the corresponding climate cells (Muñoz-Sabater et al., 2021)

3.3 Land cover changes

The Sedcas model is setup to take into account 3 types of landcover: bedrock, vegetation and glacier. To simulate the change from glacial to periglacial conditions to more vegetated conditions, a scenario will be set up where over time the area of the glaciers in the catchments decreases and the area of the vegetation increases. Initial conditions for each of the study areas will be extracted using a Normalized Difference Vegetation Index (NDVI) and Randolph Glacier Inventory (RGI) (RGI 7.0 Consortium, 2023). The decrease in glacier area will be estimated using literature and increase in vegetation cover will be estimated using a NDVI.

3.3.1 NDVI and Vegetation coverage survey

To assess the starting situation for vegetation, Landsat images from the Landsat 5 and 8 mission are used to make a Normalized Difference Vegetation Index (NDVI). NDVI makes use of two bands of Landsat, band 4: red (visible), and band 5: Near infrared (NIR) (Formula 2) (Tucker, 1979).

$$NDVI = \frac{(NIR - RED)}{(NIR + RED)} \qquad (2)$$

To assess the total area of vegetation a value of 0.1 will be used to classify the vegetation. Everything above this value is assumed to be vegetation and everything below this value is assumed to be something else. To estimate the increase in vegetation cover for the total study areas a NDVI will also be used but it will be extracted in timesteps of 1 year for 1996 to 2022 to get a trend. It is not possible to go back further in time because there is no data available. Focus will be on images with as little as possible cloud cover. Al the images that will be used need to be taken in October and ideally with only 10% cloud cover. For each year the mean surface reflection values for October for the days that meet all requirements are used for the calculation of the NDVI. Google Earth Engine (GEE) will be used to extract the images and calculate the NDVI (Gorelick et al., 2017).

3.3.2 Glacier extent and retreat

SedCas needs glacier area in percentages as input for the model. For this study glacier data has been extracted from the Randolph glacier inventory version 7 (RGI Consortium, 2023). This is a global inventory of glaciers in the form of vector outlines. This inventory includes glaciers that are larger than 0.01 km^2 and is made with the purpose of having a global dataset as close to a specific year as possible to perform large scale analysis or modelling (Pfeffer et al., 2014). For this study it is also important to have the glacier area changes for the specific study areas. There have been studies estimating the amount of glacier loss for different climate scenarios (Hugonnet et al., 2021). Most of them look at the amount of mass loss that has occurred until 2100. Unfortunately, these are not suitable for the SedCas model because it takes glacier area as input instead of glacier mass. For past glacier changes estimates from Cogley (2016) have been used. Here an assessment was done of glacier shrinkage for all of HMA based on 155 publications that reported glacier area change. Glacier area changes were estimated for 5-year periods for a 0.5° geographical grid over a timespan from 1960 until 2010. Using these glacier area changes and the glacier area in the year 2000 based on the RGI 7 a rough estimate of glacier area change can be done (Table 2).

Table 2 Area of glacier (% and km^2) in 1968 and 2000 based on Cogley (2016) and RGI7.

Study area	Glacier area 1968 (Km^2)	Glacier area 1986 (%)	RGI7 (Km^2)	Glacier area RGI7 (%)
Bagrot valley	104.1363	22.7	100	21.8
Mustang	301.6907	8.5	146	7.2
Langtang valley	163.1787	32.3	258	28.9

3.4 Landcover scenarios and climate change

SedCas has been developed and calibrated for the Illgraben catchment. The idea is to use the exact setup of Illgraben and only change land cover and the climate that the catchment is located in. The study areas are significantly larger than the Illgraben catchment resulting in more climate and landcover variability in these areas. Therefore, to see how the Illgraben catchment would respond to climate and landcover changes in these different study areas it will be moved over the different climate cells of ERA5 and landcover will be changed accordingly. The aim of this study is not to only

model the total effect of climate change and landcover change on debris flow magnitude and frequency patterns but also to get an idea of the individual changing aspects that climate and landcover change brings. Therefore, it is important to not change to many variables at once. To not make this mistake the study will have a few stages going from very conceptual to a more real-world approach.

3.4.1 Sensitivity to changes in vegetation and glacier cover

First, the model's sensitivity to changes in vegetation and glacier area have been tested. This is done by running the model for each variable separately with increases in these variables of 5 % with each step. For vegetation cover the amount of vegetation and the changes in vegetation will be based on the 10th (≈7.5%) and 90th (≈22.5%) percentile of the vegetation cover survey conducted with Google Earth Engine using an NDVI. Because the vegetation is measured in October two more steps of vegetation increase are added (32.5%), to account for higher vegetation cover in the summer months. Because there is only a small difference in the 10th percentile between all study areas, they will all have the same pattern. The glacier area sensitivity is based on the data from Kraaijenbrink et al. (2017) and Cogley (2016). The highest (32.5%) and lowest (2.5%) found glacier covers are used for the three study areas. The model will also be run for all different combinations of land uses in steps of 5% inside the bounds of the vegetation survey (7.5-32.5%) and the values provided by literature for glaciation (2.5-32.5%) (Kraaijenbrink et al., 2017; Cogley, 2016). This was only done for the climate cells as close as possible to the average climate for each study area (cells: 16 Bagrot, 33 Mustang and 21 Langtang) due to the high number of dimensions. All the changes in landcover sensitivity will be done using the full 75 years available from ERA5.

3.4.2 The effect of climate change

Secondly, the 70 years (1951-2022) available for the study areas will be divided into two climate periods of 35 years (1951-1986 and 1986-2022). This to stay with the definition of a climate which is at least a 30-year climate (Argüez & Vose, 2011). These two periods can then be compared.

3.4.2.1 Without glaciers

For the first climate comparison the model was executed for all the cells in all the study areas with a fixed land scenario. Vegetation in this scenario will be the value corresponding to the 50th percentile of the vegetation survey. There will be no glacier for this land scenarios and therefore the remaining part of the area will be bedrock.

3.4.2.2 With glaciers

For the second climate comparison the model was executed for all the cells in all the study areas with a fixed land cover scenario, this time including glacier. The value of the vegetation cover in this scenario will correspond to the 50th percentile of the vegetation survey (Appendix 1, 2 & 3), the percentage of glacier will be based on the RGI7 and the remaining part will be bedrock (Tabel 1).

3.4.2.3 With glacier and vegetation change

For the third climate comparison the model was executed for all the cells in all the study areas with changing land cover (changing vegetation and glacier area). The vegetation cover will increase from the 10th percentile to the 90th percentile of the vegetation survey (Appendix 1, 2 & 3) while the area of the glacier will decrease from the value calculated for the year 1968 to the value based on the RGI (Table 2). This to simulate what could be realistic for a vegetation change in this timespan and what is realistic for a change in glaciated area for this timespan.

3.4.3 Representative basin

3.4.3.1 Choosing representative climates

To better understand the changes in the study areas, a selection of representative basins (representative climate cells) have been chosen for each area. This because examining what is happening in every different cell is outside the possibilities of this study. However, taking a closer look at the most characteristic cells in a system could give extra insight into the driving factors in specific areas. Two cells per study area have been chosen based on their location and their changes in debris flow activity (Figure 6). To get an idea of what is happening in both increasing (colour red in table 3) and decreasing systems (colour blue in table 3) one of each will be selected. For the location systems that mostly resemble the average climate will be selected. If a system has only an increasing or a decreasing system as in the case of Bagrot a cell with extreme debris flow activity will be selected to analyse next to the most representative cell.

Table 3: Selected climate cells based on being decreasing or increasing in debris flow yield and being close to average climate.

Bagrot cellnr.	**Mustang cellnr.**	**Langtang cellnr.**
16 (increasing system)	36 (decreasing system)	20 (decreasing system)
15 (extremes)	37 (increasing system)	29 (Increasing system)

3.4.3.3 Frequency-Magnitude for the different climates

This study will also take a closer look at the frequency magnitude relationship of debris flows for a selection of cells (Table 3). This is done to see where the changes in the systems are happening and what the distributions of these changes are. The curve will compare the two different periods with their corresponding climates and land covers. For this analysis, the most complex situation will be used with changing climates and changing land cover. The comparison will be based on a cumulative frequency magnitude relation of all the debris flow events (Iacoletti et al., 2021). Specific attention will be given to the 30-year return period. This is because the total period that is examined is 35 years, and it is expected that the largest changes will be on the higher end of the curve.

4 Results

To get a better understanding of what happens in a transport limited system that is under the influence of climate change and the attributed landcover changes the model was run for a couple of different scenarios. Firstly, the effect of climate change was investigated for all three regions (4.1). Then, the model was run for 70 years where the main focus was the effect of landcover changes (4.2). After that the main focus was the combination of climate change and land cover changes where two 35 year periods where compared to see the effect of all these changes (4.3, 4.4 & 4.5). And lastly a closer look at some areas of interest was taken to mainly focus on the frequency and magnitude of debris flows (4.6).

4.1 Climate comparison

4.1.1 Temperature

As can be seen in Figures 3, 4 and 5, the average temperature is increasing over all study areas. When comparing the specific two 35-year periods this trend is still clearly visible (Table 4). The temperature increase is largest for Bagrot with 0.022 °C per year, then Mustang with 0.019 °C per year and smallest for Langtang with 0.0083 °C per year. Even though the internal variation of the average temperature between the climate cells is quite large the change in average temperature between the cells is quite consistent with a standard deviation of $3.0*10^{-3}$ °C per year for Bagrot $3.8*10^{-3}$ °C per year Mustang and $3.2*10^{-3}$ °C per year.

Table 4 Average temperature change (°C) between the periods 1951-1986 and 1986-2022 for Bagrot, Mustang and Langtang based on ERA5-land data (Muñoz-Sabater et al., 2021).

	Average temperature change (°C)		
	Bagrot	Mustang	Langtang
1951-1986	-7.69	-4.81	-3.10
1986-2022	-6.91	-4.13	-2.81

4.1.2 Precipitation

When looking at the average monthly precipitation of 1951-1986 compared to 1986-2022, a slight decrease can be seen for each study area. These decreases are small and there are no large interannual changes, however, the variability in change between the climate cells is large and not uniform, with some climate cells increasing in precipitation and some decreasing in precipitation. This can also be seen in the standard deviation of the change in precipitation between the cells. For Bagrot this is 0.54 mm, for Mustang 0.84 mm and for Langtang 2.69 mm (Table 5).

Table 5: Average precipitation change (mm/month) between the periods 1951-1986 and 1986-2022 for Bagrot, Mustang and Langtang based on ERA5-land data (Muñoz-Sabater et al., 2021).

	Average precipitation changes **(mm/month)**		
	Bagrot	Mustang	Langtang
1951-1986	77.35	74.59	163.39
1986-2022	76.69	73.14	162.61

When comparing the extreme events between the periods 1951-1986 and 1986-2022, greater differences can be seen. Precipitation above 3 mm per hour decreases for Langtang and Mustang while for Bagrot the amount of times precipitation exceeds 3 mm per hour increases. Precipitation above 5 mm per hour decreases significantly for all 3 study areas (Table 6).

Table 6: Occurrence of greater than 3 mm and 5 mm per hour rainfall intensities between the periods 1951-1986 and 1986-2022 for Bagrot, Mustang and Langtang.

	Bagrot		**Mustang**		**Langtang**	
	1951-1986	1986-2022	1951-1986	1986-2022	1951-1986	1986-2022
Pr >3 mm*h $^{-1}$	16	29	266	218	1290	1182
Pr >5 mm*h $^{-1}$	2	1	58	35	343	227

4.2 Landcover change

When running the model for the three different study areas all with their own climates and only changing the percent of vegetation cover in increments of 5% a clear negative trend can be seen. For Bagrot an increase of 5% in vegetation cover on average results in a decrease of -26.9 ± 16.6% debris flow yield, for mustang it results in a decrease of -15.5 ± 2.2%, and for Langtang it results in a decrease of -13.3 ± 2.3%. The decrease in debris flow yield seems to be largest if the climate cell has an overall higher debris flow activity. There also seems to be a link between the elevation and debris flow yield, with an optimum for debris flow yield around 4000 m for all the study areas. However, the corelation between elevation and debris flow yield is not that clear. For the highest elevations, no debris flow yield is present. Therefore, there is no visible decrease in debris flow yield with increasing vegetation cover, but there is also no increase either (Figure 7).

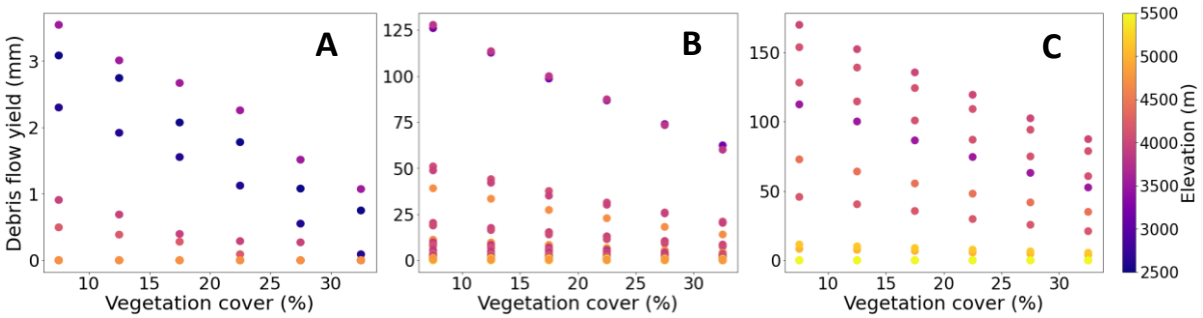

Figure 7: A-C: The amount of debris flow yield (mm/year) plotted against vegetation cover (%) and elevation (m) for Bagrot (A), Mustang (B) and Langtang (C).

The effect of increasing glacier cover has the opposite effect compared to an increase in vegetation cover. Depending on the location the trend can be non existing, linear, or exponentially increasing with increasing glacier cover (Figure 8). There is an exceptionally large variation in the response to glacier cover change. For the higher elevations, no change in debris flow activity is observed. At lower elevations, where debris flow yield is larger to begin with, the effect is larger. There also seems to be a trend between the amount of glacier melt and the debris flow yield. In both Bagrot and Mustang the largest amount of debris flow yield is produced with the largest amount of glacier melt (Figure $8_{A,B}$). However, this is not the only contributor because for Langtang the largest amount of glacier melt does not produce the largest debris flow yield (Figure 8_{C}). For the lower elevations there also seems to be a strong correlation between an increase in glacier cover and an increase in yearly average glacier melt (Figure $8_{D,E,F}$). For the higher elevation, this is not the case. Here, the yearly average glacier melt remains the same with increasing glacier cover. Except for Bagrot, where there is a very small decrease at high elevations (Figure 8_{D}).

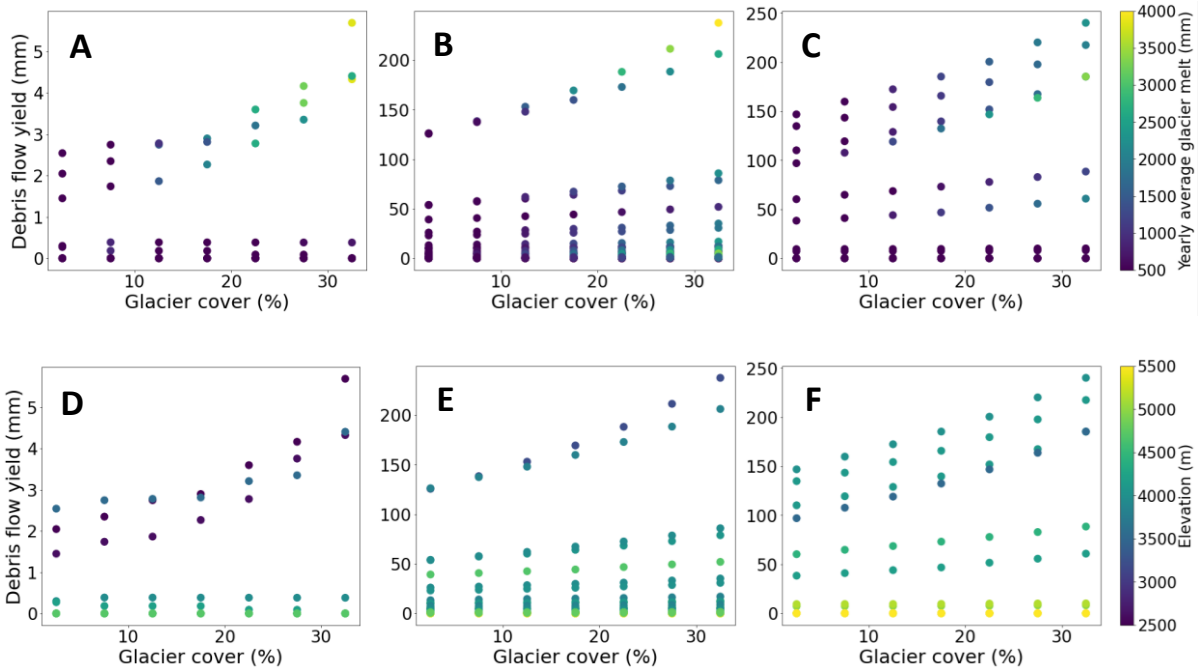

Figure 8: A-C: The amount of debris flow yield (mm/year) plotted against glacier cover (%) and yearly average glacier melt (mm) for Bagrot (A), Mustang (B) and Langtang (C). D-F: The amount of debris flow yield (mm/year) plotted against glacier cover (%) and elevation (m) for Bagrot (D), Mustang (E) and Langtang (F).

The effect of landcover change for vegetation and glaciation shows that in an active system such as Langtang and Mustang high percentages of glaciation combined with low percentages of vegetation will give an optimum situation for debris flows. Low percentages of glaciation in combination with high percentages of vegetation give significantly lower debris flow yield amounts (Figure 9_{BC}). In less active systems this is partly true. For Bagrot the overall amount of debris flow yield products is significantly less than for the other two study areas (Figure 9_{A}). And when vegetation cover gets above a certain value (22.5%) the effect of glaciation for this system is reversed. Below this value, the system reacts mostly the same as Mustang and Langtang except for the combination of 12.5% vegetation and 32.5% glacier cover, where the system behaves differently than expected.

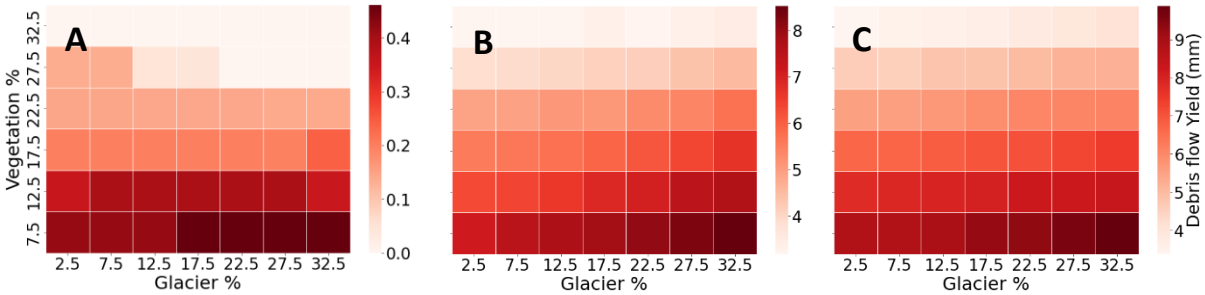

Figure 9: A-C: Heatmap of Vegetation (%) Glacier (%) and Debris flow Yield (mm) for Bagrot (A), Mustang (B) and Langtang (C)

4.3 Effect of climate change in combination with landcover

To evaluate the effect of climate change on debris flow yield in a transport-limited system the model was run for two different periods of 35 years to simulate a change in climate. In this part, three different scenarios will be discussed and compared. First, a scenario with fixed vegetation and no glaciers will be described, to only look at the effect of climate change (4.3.1). Then a scenario with fixed vegetation but also fixed glaciers will be described and compared to the previously mentioned scenario to see the effect of climate change and glaciers (4.3.2). And lastly last scenario where vegetation and glaciers change in combination with climate change will be described and compared to the other scenarios to show the whole picture (4.3.3).

4.3.1 Effect of climate change without glaciers

In systems where only the climate changes and there are no glaciers or changes in vegetation the first thing to notice is that for all systems the period during which a debris flow can occur gets longer going from May-Nov to Apr-Dec for Mustang and Langtang (Figure $10_{B,C,E,F}$). For Bagrot it increases from Jun-Aug to May-Oct (Figure $10_{A,D}$). For Bagrot the debris flow yield increases, with most of the areas going from no debris flow yield to some debris flow yield. The output of the area that already had some debris flow yield increases as well, but mostly in width (Figure $10_{A,D}$). The total average increase of debris flow yield is 0.84 mm for Bagrot. For Mustang and Langtang the debris flow yield decreases overall (Figure $10_{B,C,E,F}$). For Mustang, the total average decrease of debris flow yield is -5.33 mm, for Langtang this is -23.37 mm. It needs to be mentioned that for Mustang there are locations with a strong decrease as well as locations with an increase.

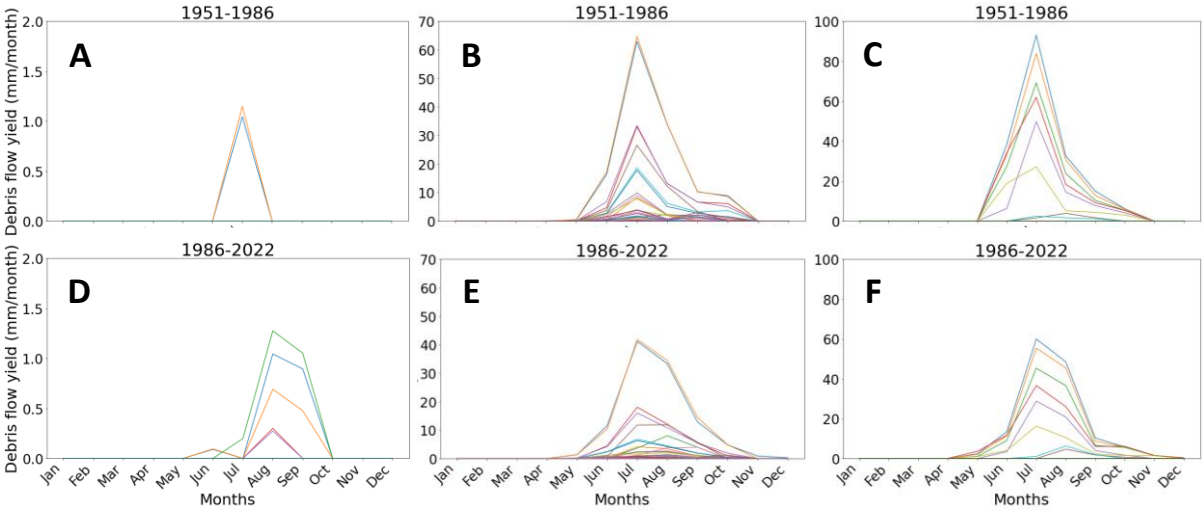

Figure 10: A-C: The average debris flow yield (mm/month) for the period 1951-1986 for each climate cell in Bagrot (A), Mustang (B) and Langtang (C), D-F: The average debris flow yield (mm/month) for the period 1986-2022 for each climate cell in Bagrot (D), Mustang (E) and Langtang (F).

It becomes noticeably clear that these three areas in HMA are quite different. Therefore, they produce different amounts of debris flow yield, and the systems also react differently to changing climate conditions. All three regions have locations where no debris flows are triggered (Figure 11). These areas are located in regions with higher elevations (Figure 12), subsequently, these are the regions that are mostly not changing. Bagrot is the only area where there is no decrease in the total amount of debris flow yield (Figure 11_{A}). While for Langtang and Mustang below an elevation of 4500 m the amount of debris flow yield produced in the system seems to decrease (Figure $11_{B,C}$). Mustang seems to have the climate cell with the largest increase in debris flow yield (11.0 mm/year) while Langtang has the one with the largest decrease in debris flow yield (-42.99 mm/year) (Figure $11_{B,C}$).

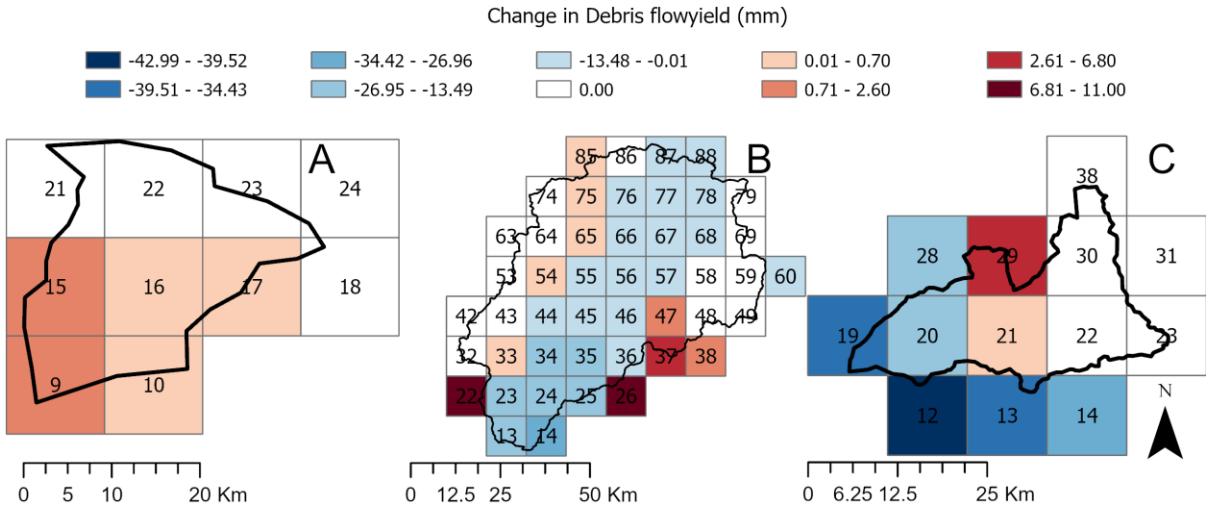

Figure 11: A-C: Change in Debris flow yield (mm/year) due to climate change for Bagrot (A), Mustang (B) and Langtang (C).

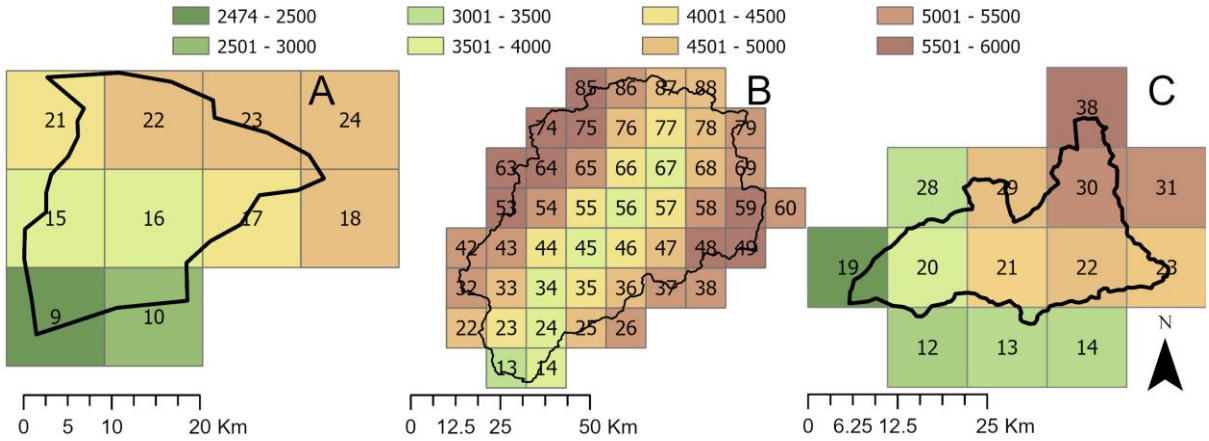

Figure 12: A-C: Elevation (m) for Bagrot (A), Mustang (B) and Langtang (C), based on ERA5-land geopotential (Muñoz-Sabater et al., 2021)

4.3.2 Effect of climate change in a cathment with glaciers

In a system with glaciers the total debris flow yield is significantly higher than without the glacier (Table 7). For Bagrot the total debris flow yield is on average 0.36 ± 0.62 mm higher, for Mustang it is 1.48 ± 4.00 mm and for Langtang it is 45.37 ± 34.94 mm higher than without glaciers. The addition of glaciers has a wide variation of effects, as the high standard deviations show. Even though the glaciers seem to have a significant effect on debris flow yield, the shape of the output graphs seems to be quite similar to the output graphs where there were no glaciers (Figures 12 & 13). The absolute change in debris flow yield between the two timesteps does not change much either (Table 7).

Table 7: Comparison of total average debris flow yield (mm/month) between catchments with and without glaciers.

	Total average debris flow yield (mm/month)				**Change in debris flow yield 1951-1986 and 1986-2022 (mm)**	
Area	1951-1986 without glaciers	1951-1986 with glaciers	1986-2022 without glaciers	1986-2022 with glaciers	Without glaciers	With glaciers
Bagrot	0.44	0.47	1.28	1.97	0.84	1.50
Mustang	18.36	19.80	13.28	14.55	-5.05	-5.25
Langtang	96.29	143.91	72.92	116.05	-23.37	-27.86

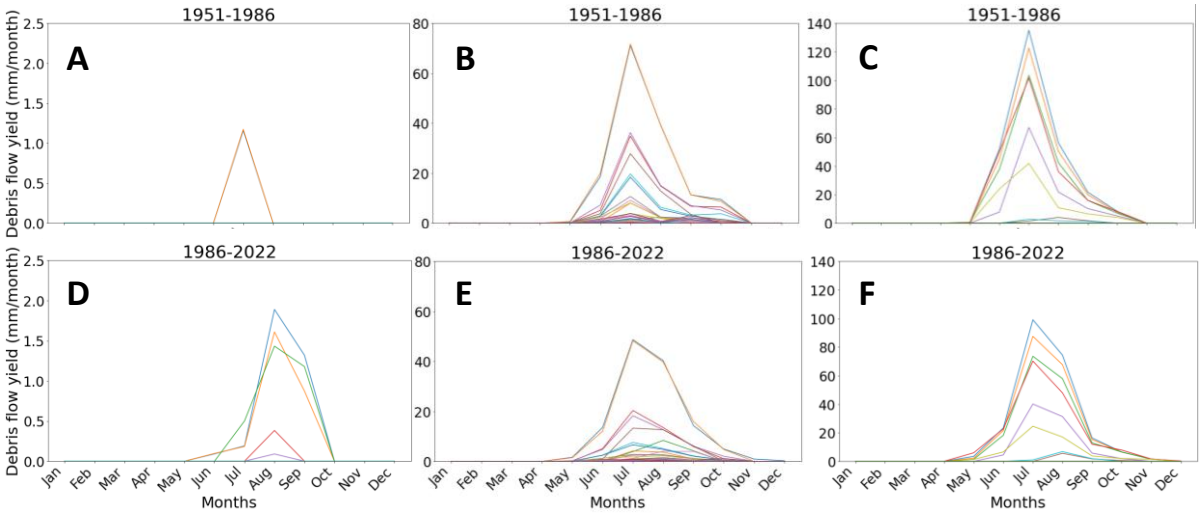

Figure 13: A-C: The average debris flow yield (mm/month) when glaciers are incorporated into the model for the period 1951-1986 for Bagrot (A), Mustang (B) and Langtang (C), D-F: The average debris flow yield (mm/month) when glaciers are incorporated into the model for the period 1986-2022 for Bagrot (D), Mustang (E) and Langtang (F).

When looking at the spatial distribution of the different climate cells the pattern has a close resemblance to the system without glaciers (Figure 14). The addition of glaciers has had a positive effect on the increasing and decreasing systems in Bagrot, Mustang and Langtang. This results in a stronger increase for systems with increasing debris flow yields and a stronger decrease in the systems with decreasing debris flow yields. There is no change in the systems that were also not active in the situation without glaciers. Langtang still has the climate cell with the strongest decrease in debris flow yield (-48.39 mm/year) and Mustang still has the one with the strongest increase (12 mm/year) (Figure $14_{B,C}$).

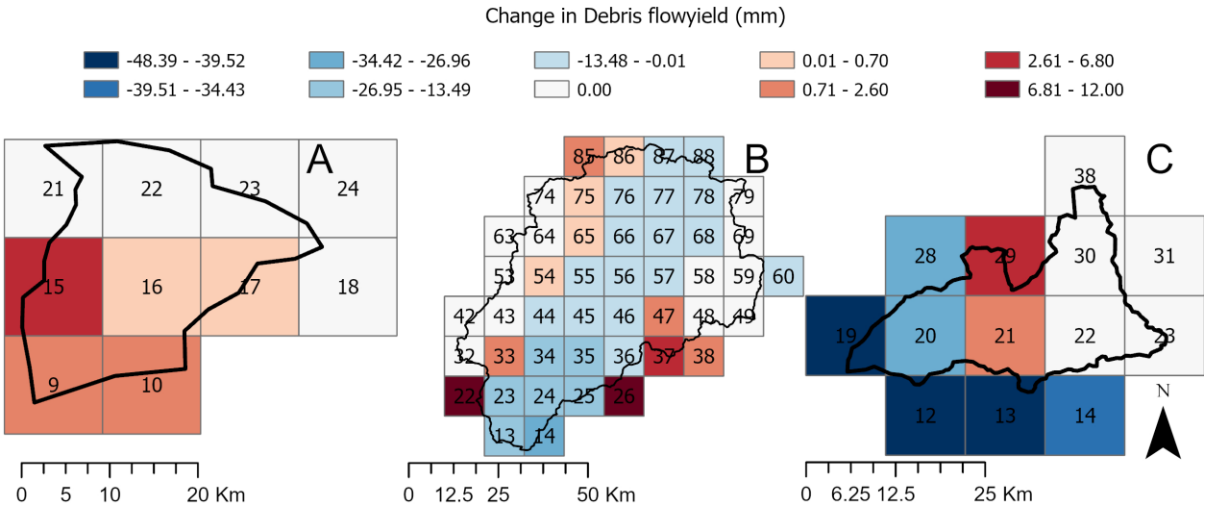

Figure 14: A-C: Change in Debris flow yield (mm/year) due to climate change with glaciers in the system for Bagrot (A), Mustang (B) and Langtang (C).

4.3.3 Effect of climate change in a cathment with landcover changes

When taking into account glacier retreat and greening of the mountains, a large overall decreasing effect can be seen for Mustang and Langtang compared to the systems where there is no landcover change. For Bagrot, the activities of the system are still increasing (Table 8). The shapes of the output graphs are again the same as for the systems without landcover change. For Bagrot, however, there is already activity in October in the time period 1951-1986 while this was not the case in the systems without land cover change. The active period of debris flow output is therefore also different for Bagrot (1951-1986) but for all the others the active period remains almost the same.

Table 8: Comparison of total average debris flow yield (mm/month) between systems with fixed landcover and with changing landcover (increasing vegetation and decreasing glacier area).

	Total average debris flow yield (mm/month)				**Change in debris flow yield 1951-1986 and 1986-2022 (mm)**	
Area	1951-1986 with fixed landcover	1951-1986 landcover change	1986-2022 with fixed landcover	1986-2022 landcover change	With fixed landcover	With landcover change
Bagrot	0.47	0.82	1.97	1.81	1.50	1.00
Mustang	19.80	22.89	14.55	11.66	-5.25	-11.23
Langtang	143.91	126.11	116.05	66.11	-27.86	-59.99

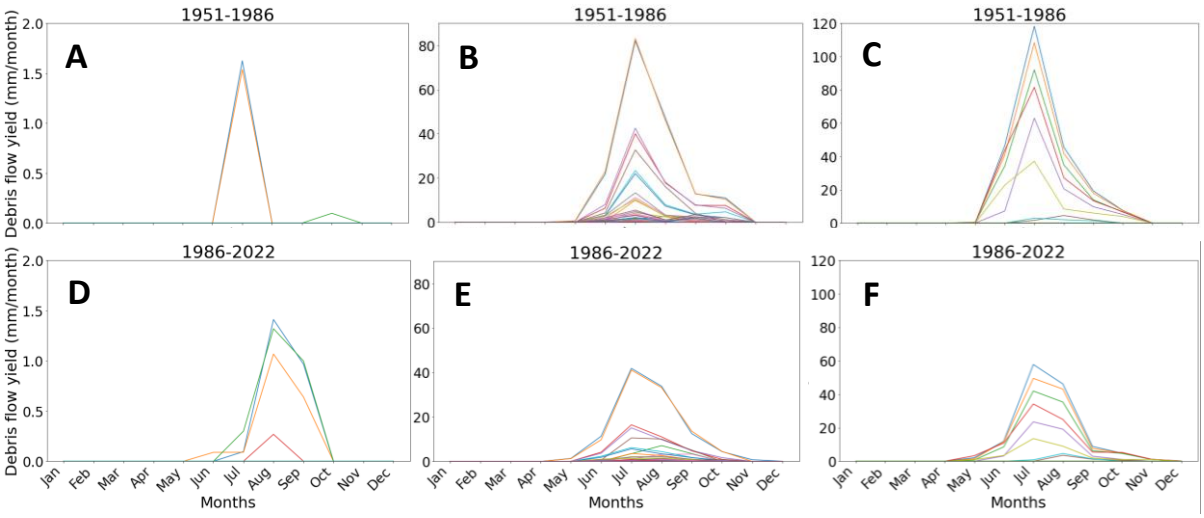

Figure 15: A-C: The average debris flow yield (mm/month) with changing landcover for the period 1951-1986 for Bagrot (A), Mustang (B) and Langtang (C), D-F: The average debris flow yield (mm/month) with changing landcover for the period 1986-2022 for Bagrot (D), Mustang (E) and Langtang (F).

The most notable effect is that some cells that were increasing in debris flow yield in the situation with only climate change, are now also decreasing. This is the case for cell 21 in Langtang and cells 65, 47 and 33 in Mustang. For Bagrot, cell 17 went from increasing to no change (Figure 14_A & 16_A). Langtang still has the climate cell with the strongest decrease going from -48.39 mm/year for a system with fixed glacier cover to -104.80 mm/year with changing land cover (Figure 14_C & 16_C). Mustang still has the climate cell with the strongest increase. This increase has gotten a bit smaller going from 12.0 mm/year to 8.20 mm/year (Figure 14_B & 16_B).

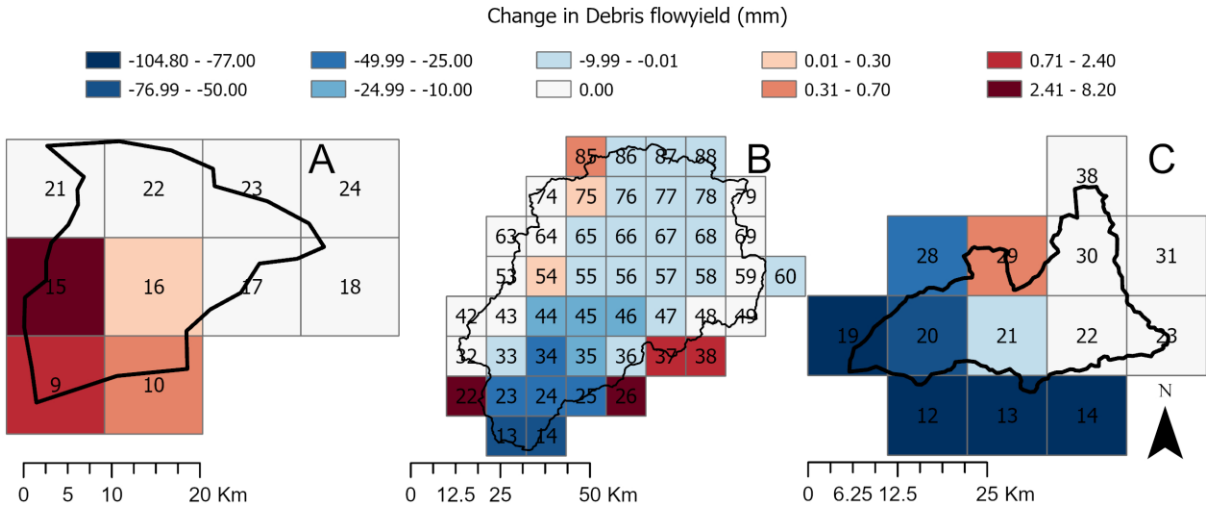

Figure 16: A-C: Change in Debris flow yield (mm/year) due to landcover change (increasing vegetation and decreasing glacier area) and climate change for Bagrot (A), Mustang (B) and Langtang (C).

4.4 Snow-covered days

There is an overall trend of a decreasing amount of snow days each year when comparing the periods 1951-1986 and 1986-2022 (Figure 17). This is the case for all 3 different study areas over the whole range of elevation. For Bagrot, the amount of snow days decreases on average with 9 days per year with a decreasing effect with increasing elevation. For Mustang, this is around 11 days, and for Langtang this is around 4.5 days. The decrease in number of snow days is larger at lower elevations than at higher elevations. At first, the decrease in the decrease is quite large, however, at some point the decrease in the number of snow days decreases only slightly with elevation and eventually it becomes zero. For Langtang and Bagrot this is at an elevation of just over 4000 m. For Mustang, this is at an elevation of 5000 m.

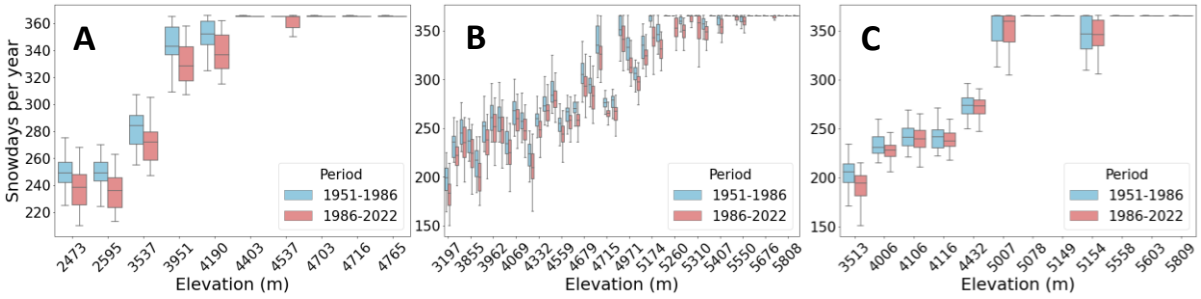

Figure 17: A-C: The average amount of snow days for the periods 1951-1986 and 1986-2022 for Bagrot (A), Mustang (B) and Langtang (C).

4.5 The relation between elevation and debris flow yield on an event basis

When plotting the debris flow yield for each event of a system with changing climate and land cover against elevation, a clear pattern arises (Figure 18). For the lower elevation, the average output per event decreases significantly between 1951-1986 and 1986-2022 for all 3 study areas, as does the output for the extreme events. For Bagrot, this is the case up to 3000 m, for Mustang up to 4900 m and for Langtang up to 5000 m of elevation. However, above these elevations an increase in the output per event can be seen. It also needs to be noted that there is a large spread in the output per event for each specific elevation.

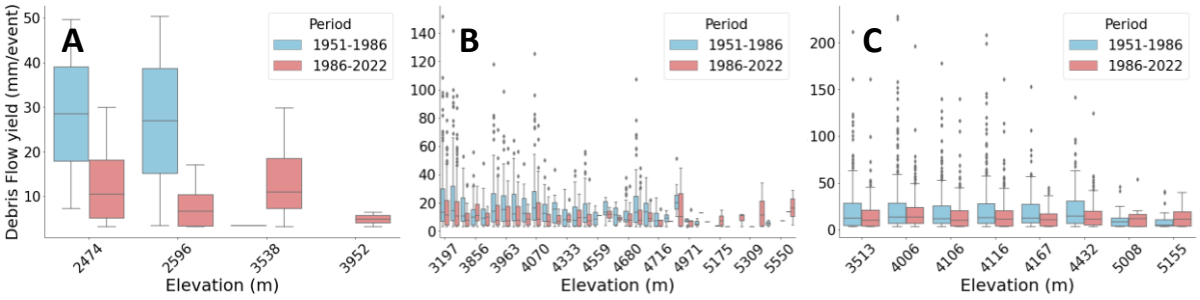

Figure 18: A-C: Debris flow yield (mm/event) plotted against elevation for Bagrot (A), Mustang (B) and Langtang (C).

4.6 Frequency magnitude relation

Bagrot has a significantly lower count of events than the other 2 study areas (Figures 19, 20 & 21). Cell 16 seems to be going from no activity to 2 debris flows in total (Figure 19_A). For this cell, for a return period of 30 years the magnitude of a debris flow event is 6.36 mm in the period 1986-2022 compared to 0 mm in the period 1951-1986. For cell 15, which has been classified as the extreme cell of the study area, it can be seen that there is a significant increase from almost no activity to more activity (Figure 19_B). The 30-year return period of this cell goes from 3.42 mm in 1951-1986 to 28.67 mm in the period 1986-2022.

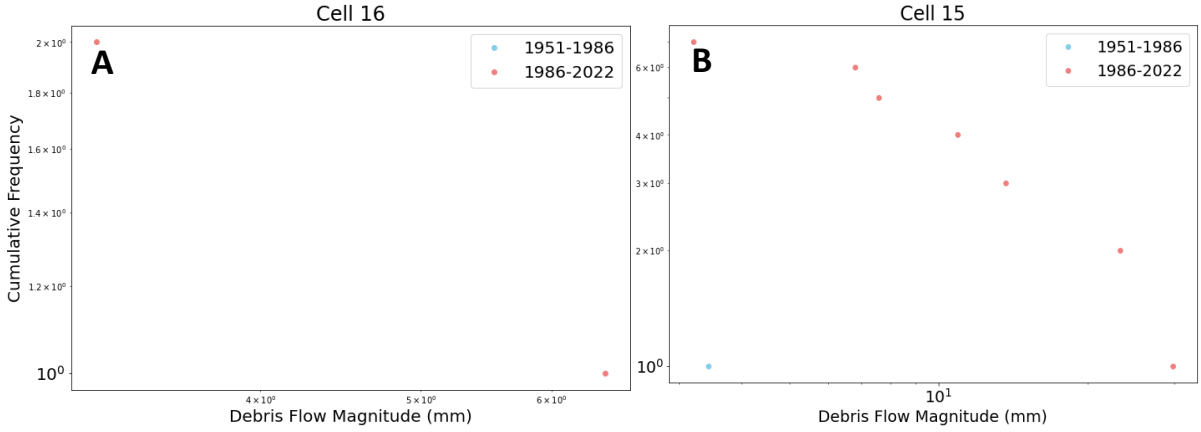

Figure 19: A-B: Cumulative frequency magnitude curve comparison between 1951-1986 and 1986-2022 for Bagrot climate cell 16 (A) and climate cell 15 (B).

Mustang has in comparison to Bagrot more activity and has cells that decrease in activity (Figures 19 & 20). For climate cell 36 there is a large shift in the whole curve meaning that the overall magnitude of the debris flows decreases significantly (Figure 20_A). Depending on the different parts of the curve it becomes clear that the decrease is not uniform, some parts decrease more than others. The 30-year return period for this cell decreases from 30.72 mm in 1951-1986 to 21.63 mm in the period 1986-2022. For climate cell 37 the same pattern can be seen as for climate cell 15 in Bagrot. Here the

system goes from almost no activity to some activity (Figure 19_B & 20_B). The 30-year return period of this cell goes from 3.77 mm in 1951-1986 to 14.99 mm in the period 1986-2022.

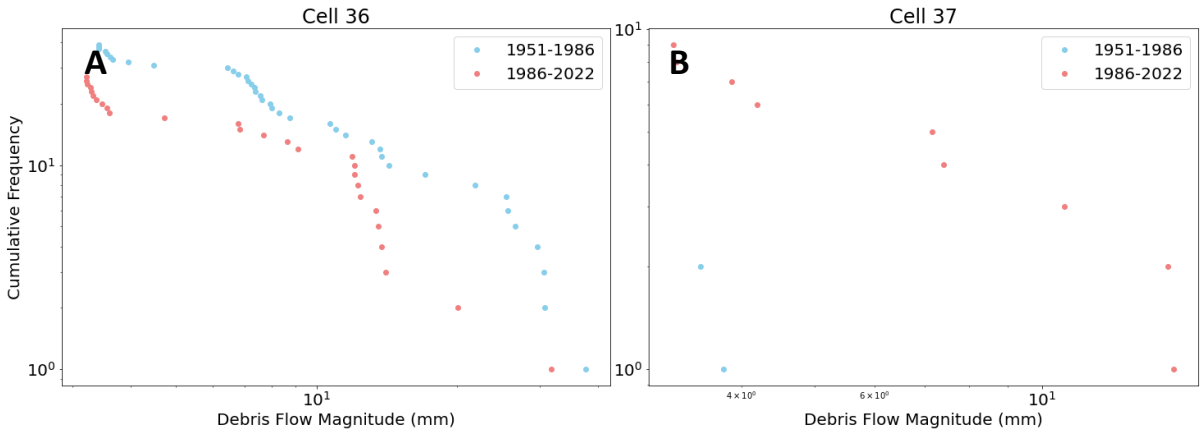

Figure 20: A-B: Cumulative frequency magnitude curve comparison between 1951-1986 and 1986-2022 for Mustang climate cell 36 (A) and climate cell 37 (B).

For Langtang, and then in particular Cell 20 a very nice curve can be seen with a very uniform shift to the left indicating that the overall magnitude of debris flows decreases in the system compared to the period 1951-1986 (Figure 21_A). It should be noted that for almost all other cells in Langtang that are decreasing in debris flow yield output this is the case. The 30-year return period for this cell decreases from 77.10 mm in 1951-1986 to 51.66 mm in the period 1986-2022. Cell 29 is again selected because of the increase in debris flow yield just like cell 37 for Mustang and cell 15 for Bagrot, however, this is a more complex curve. More to the left of the plot the events are rather similar in magnitude with the shift to the right in the middle indicating higher magnitudes for the period 1986-2022 and after that for the two highest ranked events a switch where events for 1951-1986 have a higher magnitude compared to 1986-2022 (Figure 21_B). This shows that the most extreme events decreased in magnitude but there has been an increase in magnitude for the middle extreme event. The 30-year return period of this cell goes from 39.98 mm in 1951-1986 to 37.01 mm in the period 1986-2022. This indicates the same pattern that the most extreme events decrease in magnitude.

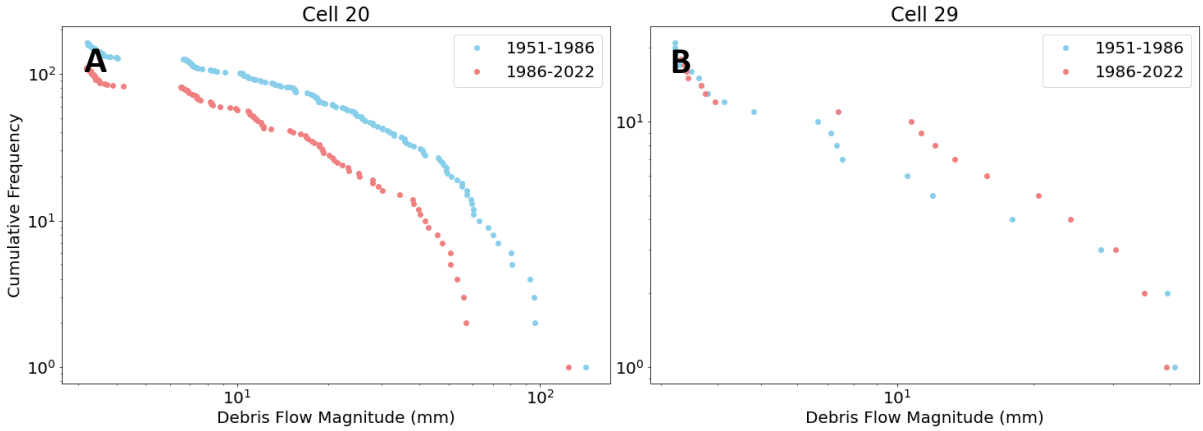

Figure 21: A-B: Cumulative frequency magnitude curve comparison between 1951-1986 and 1986-2022 for Langtang climate cell 20 (A) and climate cell 29 (B).

5 Discussion

5.1 Sedcas Model

The SedCas model was chosen for its simplicity and good performance in Illgraben, the catchment for which the model was originally made. For this study the model was adapted to incorporate glaciers. Because almost all the parameters are kept the same, this study does not represent real-world values. However, it does give an indication of how different climates affect transport-limited debris flows in the Illgraben catchment as the model has shown to perform well with minimal calibration for present but also future climate scenarios (Hirschberg et al., 2021). This study is working with 3 significantly different systems with large differences in temperature, precipitation, seasonality of the precipitation and glacier coverage. Due to the spatially lumped nature of the model, in combination with the coarse climate resolution, it prohibits the examination of spatially important phenomena, such as partial snowmelt which is a significant factor in debris flow occurrence, or the distribution of snow due to steep slopes or wind. Looking at section 4.2, it becomes very clear that vegetation plays an important role in the triggering of transport-limited debris flows. Therefore, it should be noted that the original model has a very different type of vegetation, mostly trees compared to the study areas where there is some forest, but it is mostly dominated by shrubs and grasslands (Regmi et al., 2020; Chetri & Gurung, 2004; Ali et al., 2017). This means that there might be an underestimation of the runoff due to differences in storage capacity and therefore evapotranspiration, however, this also depends on many factors (Chen et al., 2021; Bosch & Hewlett, 1982).

There is also a phenomenon in the model output where there are cells that have permanently increasing snow cover. This is not very strange because all the study areas have locations that have glaciers. However, the areas only partly match up or seem significantly larger than in reality. This can possibly be linked to the coarse resolution of ERA5 and ERA5-land, but it should also be noted that the model was not originally developed for these conditions and that even though glaciers are added to the model, this phenomenon is not linked to or the result of this addition. However, it would be a good addition to the model to link the snow accumulation to a glacier storage to have a simplified glacier mass balance instead of unlimited glacier. This was outside the scope of this study but would be of interest for future studies.

5.2 Data

5.2.1 ERA5-Land and ERA5

From this study, it becomes very clear that in these 3 study areas there is large variability in temperature and precipitation and subsequently debris flow response (Figure 3, 4, 5 & 10). However, the resolution of ERA5 land with a grid of 0.1° (9 km) is still too coarse when comparing it to Hirschberg et al. (2021) and the catchment areas used in the SedCas model of 4.83 km^2. ERA5-land also does not cover the full range of elevation in the catchments because of the coarse resolutions, mostly losing the higher elevations in the study areas (Figure 11). However, this does not matter for this case because on these high elevations temperatures are far below 0 degrees Celsius all of the time resulting in permanent snow cover inhibiting the triggering of debris flows. Another problem with the coarse resolution is also related to the snow cover and elevation changes. Due to the large elevation change in an area there might be cells that in reality have partial snow cover, however, due to the average temperature being below zero the cell in the model has total snow coverage. Which can lead to an underestimation of the debris flow yield and occurrence. For future studies, a better climate resolution would still improve the understanding of these systems. ERA5 land also does not provide any possibility to do climate predictions because it only has climate reconstructions, this significantly limits what can be done in this study. For climate predictions, for example for RCP

scenarios, another climate model should be used, but at the time of this study, no such model was available due to the need for hourly data to run the model.

5.2.2 NDVI

NDVI is the most common method to estimate vegetation coverage remotely, GEE makes this process significantly easier, faster and more reliable because of the possibility to average the values over multiple days, decreasing the effect of possible shadows or short periods of droughts (Kumar & Mutanga, 2018). However, the periodic signal of dry or wet periods over multiple years due to for example El Niño or other teleconnections could still affect the overall trend that has been acquired for this study (Kamil et al., 2019). This might be one of the reasons for the steep changes found in this study which are significantly higher than have been seen in other regions (Appendix 1, 2 &3) (Cannone et al., 2007). A longer survey period might show these more periodic changes over time. This would make it possible to normalize the increasing signal over time and make a better estimate of the increase or decrease in vegetation under the influence of climate change. However, due to the limited period satellites are operational, it is not possible to look further back in the past than 1995. The survey does provide us with a range of realistic values for the regions and the same patterns are found in other studies (Y. Liu et al., 2022; Ougahi et al., 2022). And between these bounds the effect of vegetation changes can successfully be examined.

5.2.3 Glacier area

The Randolf Glacier inventory uses part of the global land ice measurements from space (GLIMS) database and tries to portray a snapshot in time of all the glaciers over the world as close as possible to the year 2000. For some regions the time between timesteps of available data is still substantial, making the estimates less accurate. This is mostly the case in areas that are less surveyed. However, for large-scale modelling it is still the golden standard for glacier area in the year 2000 due to its global coverage (Shean et al., 2020; Zhao et al., 2014; Kraaijenbrink et al., 2017). RGI is not suitable for glacier area change. Therefore, a survey of Cogley (2016) was used. This is a meta-analysis of 155 peer-reviewed papers. Due to the coarse resolution of 0.5° which is significantly lower than the resolution of ERA5 or ERA5-land (0.25° and 0.1°), with this paper's approach some possible small-scale changes caused by topography will go unnoticed, resulting in under or overestimations of the glacier area changes (Rummukainen, 2015). However, due to the nature of this study, where the change in glacier area only needs to be a realistic value and not an exact number, this is not significant, since a far larger range of possibilities is modelled for the effect of vegetation on debris flow yield. It should also be noted that the values for the glacier area change of the past as described by Cogley (2016) are much lower than the expected glacier loss for the next century (Kraaijenbrink et al., 2017).

5.3 The sensitivity of debris flow yield to landcover changes (glacier and vegetation)

Across all different climates, it becomes very clear that vegetation has a decreasing effect on the amount of debris flow yield in transport-limited systems. The cause of this is that when the vegetation in the system increases Vwcap (the amount of water storage in SedCas) increases significantly due to deeper soils and water being captured by vegetation (Bockheim et al., 2014). This results in lower peaks of water and an overall lowering of the hydrograph resulting in less surface flow (Qs in SedCas). This water that is stored eventually leaves the system in the way of groundwater or increased evapotranspiration (Bosch & Hewlett, 1982; Ougahi et al., 2022). Glaciers have the opposite effect.

When there is a larger area covered with glaciers the hydrograph gets raised higher resulting in more overland flow. Even though glaciers are linked to temperature and fluctuate over time the contribution of the meltwater is relatively steady compared to the contribution of rainwater. The way a system reacts to the lifting or lowering of the hydrograph depends on the shape of it. If there are a few very narrow peaks, the change in overland flow and therefore in debris flow yield will be minimal. However, when the system has significant amounts of well-distributed variability, the movement of a hydrograph can have a large impact on the amount of debris flow yield. 4.3 shows the combined effect of glacier and vegetation cover. Here, it becomes clear that the patterns of Mustang and Langtang are similar (Figure $9_{B,C}$). For Bagrot this is not the case. Bagrot has significantly lower activity overall compared to Mustang and Langtang, resulting in a decreasing effect when glaciers increase (Figure 9_{A}). This phenomenon is only visible in low activity catchments when the magnitude of the system decreases to 0.2 mm of debris flow yield. When compared to a more active cell in Bagrot, the normal pattern can be observed which matches the pattern of Mustang and Langtang (Figure 22). This weird anomaly is also witnessed in other cells in Mustang that have very low activity. It was not possible to find an explanation for the anomaly and future studies that use the model should take into account that the model behaves this way. This behaviour goes against the overall expectations of the results. Landcover changes such as glacier retreat and increasing vegetation have show to be important factors for debris flow activity. Another landcover change that could be included into the model would be permafrost melting, which is a key factor in the process of going from glacial to periglacial conditions to more vegetated conditions. This addition would be especially valuable in a sediment limited system. Where melting permafrost would free up new sediment in the system (Porter et al., 2018).

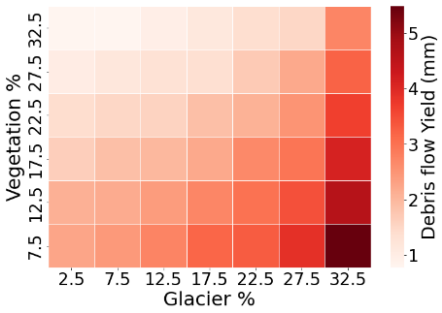

Figure 22: Heatmap of Vegetation (%) Glacier (%) and Debris flow Yield (mm) for Bagrot

5.4 The effect of climate change on debris flow yield and occurrence

The most prominent effect of climate change that is seen in this comparison of two 35-year periods is an increase in average temperature of 0.78 °C, 0.68 °C and 0.29 °C for Bagrot, Mustang and Langtang (Figure 3_B, 4_B & 5_B). This, in combination with changes in precipitation over time, changes the debris flow yield output in the systems. The most notable effects of the increasing temperature are a decrease in snow covered days and an increase of the elevation at which permanent snow cover is present (Figure 17). This is due to faster melting rates and less precipitation falling as snow in the first place (Notarnicola, 2020). Since the model is build around the notion that when there is snow cover it is impossible for debris flows to occur (Bennett et al., 2014; Bardou & Delaloye, 2004), a decrease in snow cover days increases the period wherein debris flows can take place. The decrease in snow cover days can clearly be seen in the widening of the graphs in section 4.3. While the shift in elevation at which the snow cover is permanent explains the increase in debris flow yield at higher elevations (Figure 18). The other effect that can be seen in the comparison of the two 35 years is the change in precipitation. For all 3 areas a small decrease in average monthly precipitation can be seen. However, this decrease is never more than 1.5 mm and is not expected to be the reason for the overall decreases that can be seen in debris flow yield or occurrence. The decrease in debris flow yield or occurrence is most likely due to changes in precipitation extremes (Table 6) (Kobashi et al., 2021). An increase in precipitation extremes for Bagrot resulted in an increase in debris flow yield and occurrence and for Mustang and Langtang decreases in precipitation extremes resulted in decreases in debris flow yield and occurrence. Depending on the location and its current climate,

changes in temperature or precipitation can have a larger effect and therefore the combination of those two factors is important for the outcome.

When looking at the 30-year return period of the representative basin it shows what is already expected based on all the results from section 4.1 (Figure 19, 20 & 21). However, a closer look into the magnitude frequency curves of the representative basins shows non-uniform changes in the magnitude of the different cells. There is not much to say about the curves from Bagrot except that they increase, probably due to increased precipitation extremes, increased melting and less snow (Figure 19). For Mustang cell 37 (Figure 20_B), this is also the case, however, for cell 36 (Figure 20_a) and Langtang cell 29 (Figure 21_B) a curve can be distinguished with non-uniform changes in the magnitude. For Langtang cell 20 (Figure 21_a) there is a more uniform shift in the magnitude frequency curves possibly due to an overall decrease in precipitation over all magnitudes. While the nonuniformity in the curves is possibly due to the changes in precipitation distribution. With for example the occurrence of very large extremes decreasing while middle large extremes increase as is the case for cell 29 in Langtang (Figure 21_B).

5.5 Sensitivity of the critical discharge for debris flows

Critical discharge for debris flows or Qdf is the threshold that needs to be reached for a debris flow to be triggered in the SedCas model. This is based on the amount of overland flow in the system Qs and is the main trigger for debris flows in a transport-limited system. By default, the Qdf for SedCas is based on and calibrated for the Illgraben catchment and has a value of 2.4 mm/h (Hirschberg et al., 2021). There is limited literature on Qdf values and no way to check if this is a realistic number for the areas of interest in this study, therefore, this value will be used for all modelling in the system. However, it is of interest for this study to know the sensitivity of this threshold. Therefore, to get an idea of the importance of this value the model was run for a handful of thresholds based on the 2.4 mm, taking a quart of this value, half of this value, double this value and four times this value. The model was run for all different climate cells in each study area and the landcover was based on the 50th percentile of the vegetation survey and RCI7 for the glacier area. The outcome shows a downward trend in debris flow count with increasing Qdf as expected (Figure 23). However, it also shows a very high sensitivity towards this Qdf value. Looking at the activity of the different study areas and the original Qdf of 2.4 mm all system shows very high activity. The reason for this is the exceptionally high activity in Illgraben due to high erosion rates and sediment production, which is probably not representable for these specific catchments in HMA. Therefore, it would be of interest in further studies to get a more representative Qdf for this region, if this is at all possible due to the variable nature of catchments as can already be seen between the 3 different study areas in this study.

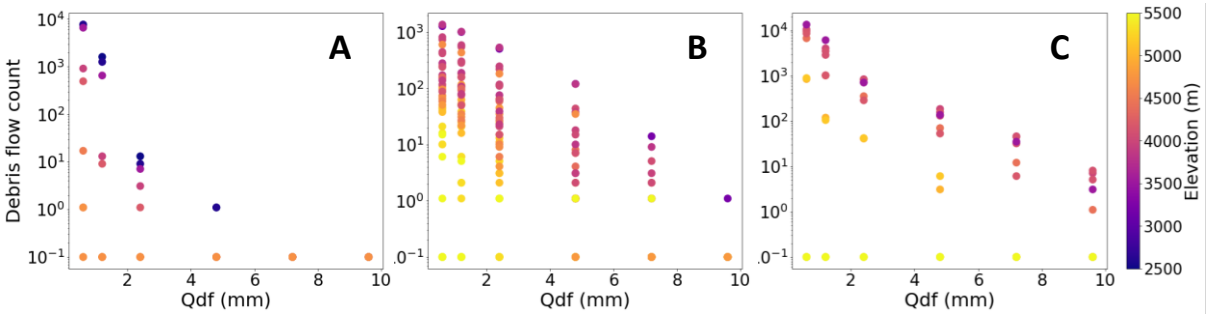

Figure 23: A-C: Debris flow count over a 70-year timespan against Qdf (mm) for Bagrot (A), Mustang (B) and Langtang (C)

5.7 Future projections and research

The model shows strong changes in debris flow activity related to climate change, but also very large variability between different regions and even inside regions. Therefore, it is hard to make predictions on how the conditions in HMA will change in the future. The overall consensus is that the average global temperature will keep rising (IPCC, 2021). Unfortunately, it is much harder to predict how precipitation patterns will change in the future, making it impossible to predict what will happen just from this study alone. Introducing future climate models into the study might give more insight into how the systems will behave in the future. For future research it might also be of interest to look at sediment limited systems. Sediment limited systems are already a part of SedCas but were outside the scope of this study. When the systems in HMA are in fact supply limited and not transport limited, climate change would probably influence the system differently. It would then be of interest to look at how mountain greening and glacier retreat affect sediment availability rather than water supply. Where glacier retreat will likely introduce a considerable amount of unconsolidated sediment to the system (increasing debris flow activity), while mountain greening would trap the sediment (decreasing debris flow activity) (Ban et al., 2020; Eichel et al., 2016). Finally, it might be useful to include other land use types such as permafrost, which would have to be added to the SedCas model. It is expected that rising temperatures melt the permafrost, freeing up extra sediment, possibly increasing debris flow activity (Porter et al., 2018).

6 Conclusions

This study shows what would happen to debris flow production of transport-limited systems if the Illgraben catchment would move over different climates in HMA. These systems are under the influence of various effects of climate change such as increasing temperatures and changing precipitation but also related effects of climate change such as glacier shrinkage and mountain greening. This study quantifies the relationship between these effects of changing climate in combination with land cover changes. This is done in the SedCas modelling framework that was originally constructed for the Illgraben catchment and is now applied to 3 regions in HMA with very different climates: Bagrot valley (Pakistan/Karakoram), the Mustang district (Himalaya/Nepal) and Langtang Valley (Himalaya/Nepal).

The results show that:

1. No large changes in yearly and monthly precipitation have been observed in this study. However, there have been some changes in the extremes of the precipitation. With decreasing rainfall extremes having a negative impact on debris flow yield production and increasing rainfall extremes having a positive impact. Increasing temperatures also change the phase in which precipitation falls. The shift from snow to rain results in shorter periods of snow cover and movement of the permanent snow cover to higher elevations. This shorter period of snow cover increases the period in which debris flows can take place. And movement of the permanent snow cover to higher elevations result in debris flows being triggered at higher elevations where it was not possible before. The temperature increase also causes an increasing amount of meltwater from glaciers. This increase in water in the systems causes an increase in the amount of debris flow yield.
2. There is a strong relationship between increasing vegetation in a system and decreasing debris flow yield. This is because the storage of a system is significantly increased resulting in less overland runoff and therefore less and less intense debris flows. The water that is captured by the vegetation leaves the system by way of increased evapotranspiration and infiltration. Decreasing glaciers has a similar effect over time. Although the amount of

meltwater increases in the short term, eventually it decreases enough to the point where less glacier means less meltwater. And this results in fewer debris flows.

3. Bagrot, Mustang and Langtang have very different climates and have very different responses to climate change. Overall, Bagrot seems to have an increase in debris flow frequency and magnitude due to increased precipitation extremes and decreased snow cover. For Langtang, the overall trend seems to be a decrease in debris flow magnitude and frequency due to a decrease in precipitation extremes in combination with increasing vegetation and decreased contribution of meltwater from glaciers. However, there are some parts of Langtang that respond differently due to some of these factors changing in a different manner. For the Mustang district, there is very large variability in response between the different climate cells. Precipitation extremes decrease overall just like in Langtang. This in combination with increasing vegetation and decreases in the contribution of meltwater from glaciers decreases the frequency and magnitude of these climate cells. However, there are regions, mostly at a higher elevation, that increase in debris flow magnitude and frequency due to a decrease in snow-covered day or a shift in the elevation of permanent snow cover.

This study confirms that climate change will have an impact on the debris flow activity in HMA. It shows how different factors like temperature, precipitation, snow cover, vegetation and glacier retreat will influence debris flow activity. And it shows how SedCas combines all these factors and can be used to predict changes in debris flow activity. Therefore, this study improves the overall understanding of debris flows. This better understanding can help the population of areas prone to debris flows to better adapt to these hazardous mass movements.

Appendix

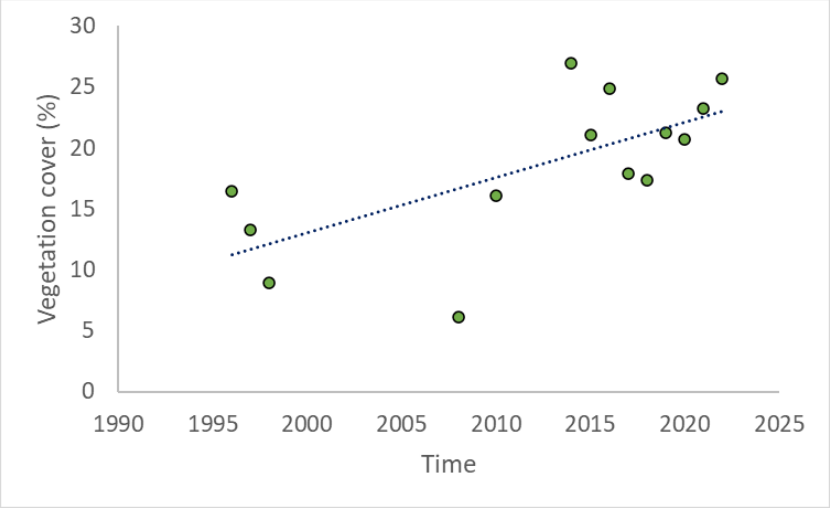

Appendix 1: Vegetation survey Bagrot valley.

Percentile	Vegetation cover (%)
10th	7.5
50th	19.3
90th	26.3

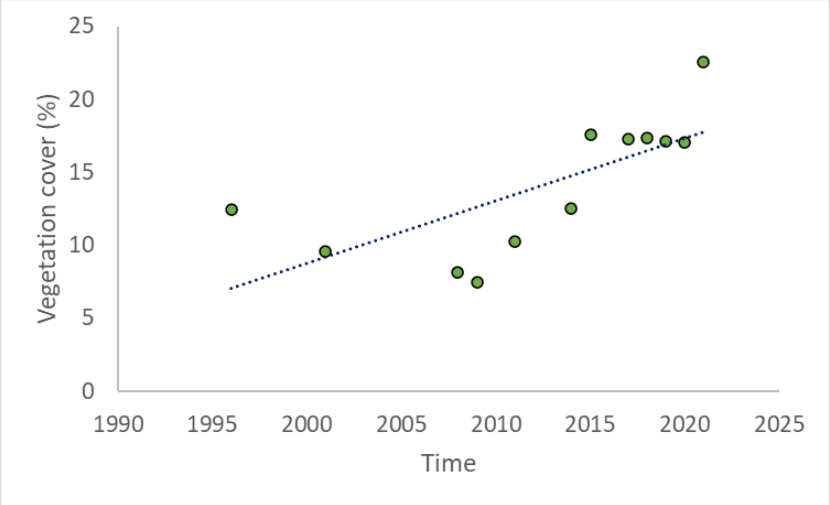

Appendix 2: Vegetation survey Mustang district.

Percentile	Vegetation cover (%)
10th	7.5
50th	19.3
90th	26.3

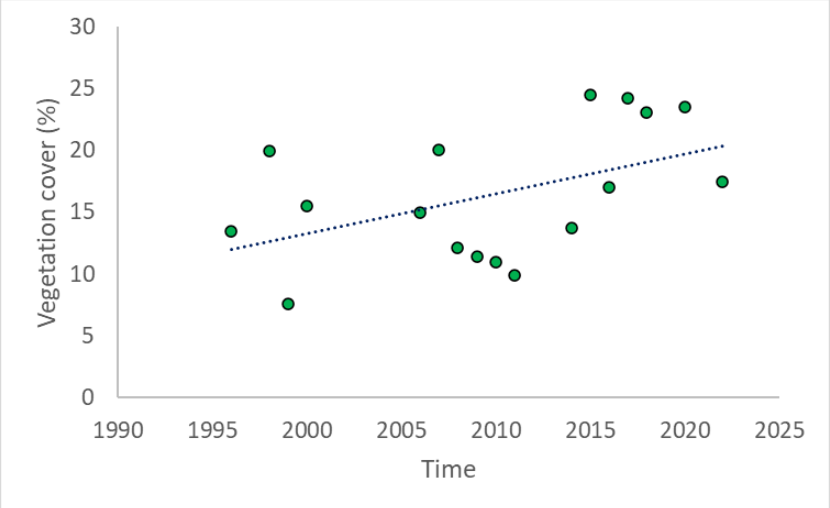

Appendix 3: Vegetation survey Langtang valley.

Percentile	Vegetation cover (%)
10th	7.5
50th	19.3
90th	26.3

References

Ali, S., Begum, F., Hayat, R., & Bohannan, B. J. M. (2017). Variation in soil organic carbon stock in different land uses and altitudes in Bagrot Valley, Northern Karakoram. *Acta Agriculturae Scandinavica Section B-soil and Plant Science*, *67*(6), 551–561. https://doi.org/10.1080/09064710.2017.1317829

Argüez, A., & Vose, R. S. (2011). The definition of the standard WMO climate normal: the key to deriving alternative climate normals. *Bulletin of the American Meteorological Society*, *92*(6), 699–704. https://doi.org/10.1175/2010bams2955.1

Bardou, E., & Delaloye, R. (2004). Effects of ground freezing and snow avalanche deposits on debris flows in alpine environments. *Natural Hazards and Earth System Sciences*, *4*(4), 519–530. https://doi.org/10.5194/nhess-4-519-2004

Bennett, G. L., Molnar, P., McArdell, B. W., & Burlando, P. (2014). A probabilistic sediment cascade model of sediment transfer in the Illgraben. *Water Resources Research*, *50*(2), 1225–1244. https://doi.org/10.1002/2013wr013806

Bhattacharya, A., Bolch, T., Mukherjee, K., King, O., Menounos, B., Kapitsa, V., Neckel, N., Yang, W., & Yao, T. (2021). High Mountain Asian glacier response to climate revealed by multi-temporal satellite observations since the 1960s. *Nature Communications*, *12*(1). https://doi.org/10.1038/s41467-021-24180-y

Bockheim, J. G., Gennadiyev, A., Hartemink, A. E., & Brevik, E. C. (2014). Soil-forming factors and Soil Taxonomy. *Geoderma*, *226–227*, 231–237. https://doi.org/10.1016/j.geoderma.2014.02.016

Bosch, J., & Hewlett, J. D. (1982). A review of catchment experiments to determine the effect of vegetation changes on water yield and evapotranspiration. *Journal of Hydrology*, *55*(1–4), 3–23. https://doi.org/10.1016/0022-1694(82)90117-2

Bovis, M. J., & Jakob, M. (1999). The role of debris supply conditions in predicting debris flow activity. *Earth Surface Processes and Landforms*, *24*(11), 1039–1054. https://doi.org/10.1002/(sici)1096-9837(199910)24:11

Brayshaw, D., & Hassan, M. A. (2009). Debris flow initiation and sediment recharge in gullies. *Geomorphology*, *109*(3–4), 122–131. https://doi.org/10.1016/j.geomorph.2009.02.021

Calligaris, C., Poretti, G., Tariq, S., & Melis, M. T. (2013). First steps towards a landslide inventory map of the Central Karakoram National Park. *European Journal of Remote Sensing*, *46*(1), 272–287. https://doi.org/10.5721/eujrs20134615

Cannone, N., Sgorbati, S., & Guglielmin, M. (2007). Unexpected impacts of climate change on alpine vegetation. *Frontiers in Ecology and the Environment*, *5*(7), 360–364. https://doi.org/10.1890/1540-9295(2007)5

Chen, Z., Wang, W., Woods, R., & Shao, Q. (2021). Hydrological effects of change in vegetation components across global catchments. *Journal of Hydrology*, *595*, 125775. https://doi.org/10.1016/j.jhydrol.2020.125775

Chetri, M., & Gurung, C. R. (2004). Vegetation composition, species performance and its relationship among the livestock and wildlife in the grassland of upper Mustang, Nepal ∗. *Session III : Nutrition and Feeds*. http://ivis.org/proceedings/yaks/2004/session3/chetri.pdf

Cogley, J. G. (2016). Glacier shrinkage across High Mountain Asia. *Annals of Glaciology*, *57*(71), 41–49. https://doi.org/10.3189/2016aog71a040

Collier, E., & Immerzeel, W. W. (2015). High-resolution modeling of atmospheric dynamics in the Nepalese Himalaya. *Journal of Geophysical Research: Atmospheres*, *120*(19), 9882–9896. https://doi.org/10.1002/2015jd023266

Costa, J.E., 1998, Rheologic, geomorphic, and sedimentologic differentiation of water floods, hyperconcentrated flows, and debris flows, in Baker, V.R., Kochel, R.C., and Patton, P.C., eds. Flood geomorphology: New York, John Wiley & Sons, p. 113-122

Coulthard, T., Ramirez, J., Fowler, H. J., & Glenis, V. (2012). Using the UKCP09 probabilistic scenarios to model the amplified impact of climate change on drainage basin sediment yield. *Hydrology and Earth System Sciences*, *16*(11), 4401–4416. https://doi.org/10.5194/hess-16-4401-2012

Eichel, J., Corenblit, D. J., & Dikau, R. (2016). Conditions for feedbacks between geomorphic and vegetation dynamics on lateral moraine slopes: a biogeomorphic feedback window. *Earth Surface Processes and Landforms*, *41*(3), 406–419. https://doi.org/10.1002/esp.3859

Fort, M. (1996). Late Cenozoic environmental changes and uplift on the northern side of the central Himalaya: a reappraisal from field data. *Palaeogeography, Palaeoclimatology, Palaeoecology*, *120*(1–2), 123–145. https://doi.org/10.1016/0031-0182(94)00038-7

Fort, M. (2000). Glaciers and mass wasting processes: their influence on the shaping of the Kali Gandaki valley (higher Himalaya of Nepal). *Quaternary International*, *65–66*, 101–119. https://doi.org/10.1016/s1040-6182(99)00039-7

Fort, M. (2014). Natural hazards versus climate change and their potential impacts in the dry, northern Himalayas: focus on the upper Kali Gandaki (Mustang District, Nepal). *Environmental Earth Sciences*, *73*(2), 801–814. https://doi.org/10.1007/s12665-014-3087-y

GADM. (n.d.). https://gadm.org/

Global Administrative Areas. (2012). GADM Database of Global Administrative Areas, Version 2.0. Retrieved September 10, 2023, from https://www.gadm.org

Gorelick, N., Hancher, M., Dixon, M., Ilyushchenko, S., Thau, D., & Moore, R. (2017). Google Earth Engine: Planetary-scale geospatial analysis for everyone. *Remote Sensing of Environment*, *202*, 18–27. https://doi.org/10.1016/j.rse.2017.06.031

Grießinger, J., Meier, W. J., & Hochreuther, P. (2021). Decreasing water availability as a threat for traditional Irrigation-Based Land-Use systems in the Mustang Himalaya/Nepal. In *Springer eBooks* (pp. 253–266). https://doi.org/10.1007/978-3-030-70238-0_8

Haeberli, W. (2013). Mountain permafrost — research frontiers and a special long-term challenge. *Cold Regions Science and Technology*, *96*, 71–76. https://doi.org/10.1016/j.coldregions.2013.02.004

Harrison, H. N., Hammond, J. C., Kampf, S. K., & Kiewiet, L. (2021). On the hydrological difference between catchments above and below the intermittent-persistent snow transition. *Hydrological Processes*, *35*(11). https://doi.org/10.1002/hyp.14411

Herreid, S., & Pellicciotti, F. (2020). The state of rock debris covering Earth's glaciers. *Nature Geoscience*, *13*(9), 621–627. https://doi.org/10.1038/s41561-020-0615-0

Hewitt, K., Gosse, J. C., & Clague, J. J. (2011). Rock avalanches and the pace of late Quaternary development of river valleys in the Karakoram Himalaya. *Geological Society of America Bulletin*, *123*(9–10), 1836–1850. https://doi.org/10.1130/b30341.1

Hirschberg, J., Fatichi, S., Bennett, G. L., McArdell, B. W., Peleg, N., Lane, S. N., Schlunegger, F., & Molnar, P. (2021). Climate change impacts on sediment yield and Debris-Flow activity in an alpine catchment. *Journal of Geophysical Research: Earth Surface*, *126*(1). https://doi.org/10.1029/2020jf005739

Huang, W., Duan, W., Nover, D., Sahu, N., & Chen, Y. (2021). An integrated assessment of surface water dynamics in the Irtysh River Basin during 1990–2019 and exploratory factor analyses. *Journal of Hydrology*, *593*, 125905. https://doi.org/10.1016/j.jhydrol.2020.125905

Hugonnet, R., McNabb, R., Berthier, É., Menounos, B., Nuth, C., Girod, L., Farinotti, D., Huss, M., Dussaillant, I., Brun, F., & Kääb, A. (2021). Accelerated global glacier mass loss in the early twenty-first century. *Nature*, *592*(7856), 726–731. https://doi.org/10.1038/s41586-021-03436-z

Iacoletti, S., Cremen, G., & Galasso, C. (2021). Advancements in multi-rupture time-dependent seismic hazard modeling, including fault interaction. *Earth-Science Reviews*, *220*, 103650. https://doi.org/10.1016/j.earscirev.2021.103650

Immerzeel, W. W., Wanders, N., Lutz, A., Shea, J. M., & Bierkens, M. F. P. (2015). Reconciling high-altitude precipitation in the upper Indus basin with glacier mass balances and runoff. *Hydrology and Earth System Sciences*, *19*(11), 4673–4687. https://doi.org/10.5194/hess-19-4673-2015

IPCC, 2021: Summary for Policymakers. In: Climate Change 2021: The Physical Science Basis. Contribution of Working Group I to the Sixth Assessment Report of the Intergovernmental Panel on Climate Change [Masson-Delmotte, V., P. Zhai, A. Pirani, S.L. Connors, C. Péan, S. Berger, N. Caud, Y. Chen, L. Goldfarb, M.I. Gomis, M. Huang, K. Leitzell, E. Lonnoy, J.B.R. Matthews, T.K. Maycock, T. Waterfield, O. Yelekçi, R. Yu, and B. Zhou (eds.)]. In Press.

Istanbulluoglu, E. (2009). Modeling Catchment Evolution: From Decoding Geomorphic Processes Signatures toward Predicting Impacts of Climate Change. *Geography Compass*, *3*(3), 1125–1150. https://doi.org/10.1111/j.1749-8198.2009.00228.x

Itakura, Y., Inaba, H., & Sawada, T. (2005). A debris-flow monitoring devices and methods bibliography. *Natural Hazards and Earth System Sciences*, *5*(6), 971–977. https://doi.org/10.5194/nhess-5-971-2005

Iverson, R. M. (1997). The physics of debris flows. *Reviews of Geophysics*, *35*(3), 245–296. https://doi.org/10.1029/97rg00426

Jakob, M. (1996). Morphometric and geotechnical controls of debris flow frequency and magnitude in Southwestern British Columbia. *British Columbia (Doctoral Dissertation, University of British Columbia)*. https://doi.org/10.14288/1.0087740

Kamil, S., Almazroui, M., Kang, I., Hanif, M. U., Kucharski, F., Abid, M. A., & Saeed, F. (2019). Long-term ENSO relationship to precipitation and storm frequency over western Himalaya–Karakoram–Hindukush region during the winter season. *Climate Dynamics*, *53*(9–10), 5265–5278. https://doi.org/10.1007/s00382-019-04859-1

Kobashi, R., Kita, M., Uchida, T., & Kawahara, Y. (2021). STUDY ON AN EVALUATION METHOD OF INITIATION PROBABILITY OF DEBRIS FLOWS DURING HEAVY RAINFALL. *Journal of JSCE*, *9*(1), 94–102. https://doi.org/10.2208/journalofjsce.9.1_94

Kraaijenbrink, P., Bierkens, M. F. P., Lutz, A., & Immerzeel, W. W. (2017). Impact of a global temperature rise of 1.5 degrees Celsius on Asia's glaciers. *Nature*, *549*(7671), 257–260. https://doi.org/10.1038/nature23878

Kraaijenbrink, P., Stigter, E. E., Yao, T., & Immerzeel, W. W. (2021). Climate change decisive for Asia's snow meltwater supply. *Nature Climate Change*, *11*(7), 591–597. https://doi.org/10.1038/s41558-021-01074-x

Kumar, L., & Mutanga, O. (2018). Google Earth Engine Applications Since Inception: Usage, Trends, and potential. *Remote Sensing*, *10*(10), 1509. https://doi.org/10.3390/rs10101509

Lacroix, P. (2016). Landslides triggered by the Gorkha earthquake in the Langtang valley, volumes and initiation processes. *Earth, Planets and Space*, *68*(1). https://doi.org/10.1186/s40623-016-0423-3

Lama, L., Kayastha, R. B., Maharjan, S. B., Bajracharya, S. R., Chand, M. B., & Mool, P. K. (2015). Glacier area and volume changes of Hidden Valley, Mustang, Nepal from ~1980s to 2010 based on remote sensing. *Proceedings of IAHS*, *368*, 57–62. https://doi.org/10.5194/piahs-368-57-2015

Legg, N. T., Meigs, A., Grant, G. E., & Kennard, P. (2014). Debris flow initiation in proglacial gullies on Mount Rainier, Washington. *Geomorphology*, *226*, 249–260. https://doi.org/10.1016/j.geomorph.2014.08.003

Liu, Y., Li, Z., Chen, Y., Kayumba, P. M., Wang, X., Liu, C., Long, Y., & Sun, F. (2022). Biophysical impacts of vegetation dynamics largely contribute to climate mitigation in High Mountain Asia. *Agricultural and Forest Meteorology*, *327*, 109233. https://doi.org/10.1016/j.agrformet.2022.109233

Liu, Z., Wang, Y., Xu, Z., & Duan, Q. (2017). Conceptual Hydrological Models. In *Springer eBooks* (pp. 1–23). https://doi.org/10.1007/978-3-642-40457-3_22-1

Maina, F. Z., Kumar, S. V., Albergel, C., & Mahanama, S. (2022). Warming, increase in precipitation, and irrigation enhance greening in High Mountain Asia. *Communications Earth & Environment*, *3*(1). https://doi.org/10.1038/s43247-022-00374-0

Mayer, C., Lambrecht, A., Mihalcea, C., Belò, M., Diolaiuti, G., Smiraglia, C., & Bashir, F. (2010). Analysis of glacial meltwater in Bagrot Valley, Karakoram. *Mountain Research and Development*, *30*(2), 169–177. https://doi.org/10.1659/mrd-journal-d-09-00043.1

Montgomery, D. R., & Bierman, P. R. (2013). *Key concepts in Geomorphology*. http://ci.nii.ac.jp/ncid/BB16826452

Muñoz-Sabater, J., Dutra, E., Agustí-Panareda, A., Albergel, C., Arduini, G., Balsamo, G., Boussetta, S., Choulga, M., Harrigan, S., Hersbach, H., Martens, B., Miralles, D. G., Piles, M., Rodriguez-fernandez, N., Zsótér, E., Buontempo, C., & Thépaut, J. (2021). ERA5-Land: a state-of-the-art global reanalysis dataset for land applications. *Earth System Science Data*, *13*(9), 4349–4383. https://doi.org/10.5194/essd-13-4349-2021

Nie, Y., Pritchard, H. D., Liu, Q., Hennig, T., Wang, W., Wang, X., Liu, S., Nepal, S., Samyn, D., Hewitt, K., & Chen, X. (2021). Glacial change and hydrological implications in the Himalaya and Karakoram. *Nature Reviews Earth & Environment*, *2*(2), 91–106. https://doi.org/10.1038/s43017-020-00124-w

Notarnicola, C. (2020). Observing Snow Cover and Water Resource Changes in the High Mountain Asia Region in Comparison with Global Mountain Trends over 2000–2018. *Remote Sensing*, *12*(23), 3913. https://doi.org/10.3390/rs12233913

Ougahi, J. H., Cutler, M. E. J., & Cook, S. J. (2022). Assessment of climate change effects on vegetation and river hydrology in a semi-arid river basin. *PLOS ONE*, *17*(8), e0271991. https://doi.org/10.1371/journal.pone.0271991

Pepin, N., Arnone, E., Gobiet, A., Haslinger, K., Kotlarski, S., Notarnicola, C., Palazzi, E., Seibert, P., Serafin, S., Schöner, W., Terzago, S., Thornton, J., Vuille, M., & Adler, C. (2022). Climate changes and their elevational patterns in the mountains of the world. *Reviews of Geophysics*, *60*(1). https://doi.org/10.1029/2020rg000730

Perron, J. T. (2017). Climate and the pace of erosional landscape evolution. *Annual Review of Earth and Planetary Sciences*, *45*(1), 561–591. https://doi.org/10.1146/annurev-earth-060614-105405

Pfeffer, W. T., Arendt, A. A., Bliss, A., Bolch, T., Cogley, J. G., Gardner, A., Hagen, J. O., Hock, R., Kaser, G., Kienholz, C., Miles, E., Moholdt, G., Mölg, N., Paul, F., Radić, V., Rastner, P., Raup, B. H., Rich, J., & Sharp, M. (2014). The Randolph Glacier Inventory: a globally complete inventory of glaciers. *Journal of Glaciology*, *60*(221), 537–552. https://doi.org/10.3189/2014jog13j176

Pierson, T. C. (2005). Distinguishing between debris flows and floods from field evidence in small watersheds. *U.S. GEOLOGICAL SURVEY, REDUCING RISK FROM VOLCANO HAZARDS*. https://doi.org/10.3133/fs20043142

Porter, P. R., Smart, M. J., & Irvine-Fynn, T. (2018). Glacial sediment stores and their reworking. In Geography of the physical environment (pp. 157–176). https://doi.org/10.1007/978-3-319-94184-4_10

RGI 7.0 Consortium, 2023. Randolph Glacier Inventory - A Dataset of Global Glacier Outlines, Version 7.0. Boulder, Colorado USA. NSIDC: National Snow and Ice Data Center. doi:10.5067/f6jmovy5navz. Online access: https://doi.org/10.5067/f6jmovy5navz

Rapp, A. (1960). Recent development of mountain slopes in Kärkevagge and surroundings, northern Scandinavia. *Geografiska Annaler*, *42*(2–3), 65–200. https://doi.org/10.1080/20014422.1960.11880942

Regmi, R., Ma, Y., Ma, W., Baniya, B., & Bashir, B. (2020). Interannual Variation of NDVI, Precipitation and Temperature during the Growing Season in Langtang National Park, Central Himalaya, Nepal. *Applied Ecology and Environmental Sciences*, *8*(5), 218–228. https://doi.org/10.12691/aees-8-5-5

Rheological properties. (2007). In *Food Physics. Springer eBooks* (pp. 117–206). https://doi.org/10.1007/978-3-540-34194-9_4

Rummukainen, M. (2015). Added value in regional climate modeling. *WIREs Climate Change*, *7*(1), 145–159. https://doi.org/10.1002/wcc.378

Salzmann, N., Nötzli, J., Hauck, C., Gruber, S., Hoelzle, M., & Haeberli, W. (2007). Ground surface temperature scenarios in complex high-mountain topography based on regional climate model results. *Journal of Geophysical Research*, *112*(F2). https://doi.org/10.1029/2006jf000527

Seppi, R., Zanoner, T., Carton, A., Bondesan, A., Francese, R., Carturan, L., Zumiani, M., Giorgi, M., & Ninfo, A. (2015). Current transition from glacial to periglacial processes in the Dolomites (South-Eastern Alps). *Geomorphology*, *228*, 71–86. https://doi.org/10.1016/j.geomorph.2014.08.025

Shean, D., Bhushan, S., Montesano, P., Rounce, D., Arendt, A. A., & Osmanoğlu, B. (2020). A systematic, regional assessment of High Mountain Asia glacier mass balance. *Frontiers in Earth Science*, *7*. https://doi.org/10.3389/feart.2019.00363

Singh, P., Kumar, N., & Arora, M. (2000). Degree–day factors for snow and ice for Dokriani Glacier, Garhwal Himalayas. *Journal of Hydrology*, *235*(1–2), 1–11. https://doi.org/10.1016/s0022-1694(00)00249-3

Singh, P., Spitzbart, G., Hübl, H., & Weinmeister, H. W. (1997). Hydrological response of snowpack under rain-on-snow events: a field study. *Journal of Hydrology*, *202*(1–4), 1–20. https://doi.org/10.1016/s0022-1694(97)00004-8

Steiner, J., Gurung, T. R., Joshi, S., Koch, I., Saloranta, T., Shea, J., Shrestha, A. B., Stigter, E. E., & Immerzeel, W. W. (2021). Multi-year observations of the high mountain water cycle in the Langtang catchment, Central Himalaya. *Hydrological Processes*, *35*(5). https://doi.org/10.1002/hyp.14189

Takahashi, T. (1981). Debris flow. *Annual Review of Fluid Mechanics*, *13*(1), 57–77. https://doi.org/10.1146/annurev.fl.13.010181.000421

Tucker, C. J. (1979). Red and photographic infrared linear combinations for monitoring vegetation. *Remote Sensing of Environment*, *8*(2), 127–150. https://doi.org/10.1016/0034-4257(79)90013-0

University Utrecht Login from Home. (n.d.-a). https://www-jstage-jst-go-jp.proxy.library.uu.nl/article/journalofjsce/9/1/9_94/_pdf/-char/en

University Utrecht Login from Home. (n.d.-b). https://www-jstage-jst-go-jp.proxy.library.uu.nl/article/journalofjsce/9/1/9_94/_pdf/-char/en

University Utrecht Login from Home. (n.d.-c). https://www-jstage-jst-go-jp.proxy.library.uu.nl/article/journalofjsce/9/1/9_94/_pdf/-char/en

Verbunt, M., Gurtz, J., Jasper, K., Herbert, L., Warmerdam, P., & Zappa, M. (2003). The hydrological role of snow and glaciers in alpine river basins and their distributed modeling. *Journal of Hydrology*, *282*(1–4), 36–55. https://doi.org/10.1016/s0022-1694(03)00251-8

Wake, C. P. (1989). Glaciochemical investigations as a tool for determining the spatial and seasonal variation of snow accumulation in the central Karakoram, northern Pakistan. *Annals of Glaciology*, *13*, 279–284. https://doi.org/10.1017/s0260305500008053

Wang, L., Good, S. P., & Caylor, K. K. (2014). Global synthesis of vegetation control on evapotranspiration partitioning. *Geophysical Research Letters*, *41*(19), 6753–6757. https://doi.org/10.1002/2014gl061439

Winiger, M., Gumpert, M., & Yamout, H. (2005). Karakorum-Hindukush-western Himalaya: assessing high-altitude water resources. *Hydrological Processes*, *19*(12), 2329–2338. https://doi.org/10.1002/hyp.5887

Zhao, L., Ding, R., & Moore, J. C. (2014). Glacier volume and area change by 2050 in high mountain Asia. *Global and Planetary Change*, *122*, 197–207. https://doi.org/10.1016/j.gloplacha.2014.08.006